University of Kerbala

College of Science

Department of Physics

Identification of Effective Oral Contrast Agents for Gastrointestinal Magnetic Resonance Imaging

A Dissertation Submitted to the Council of the College of Science, University of Kerbala, in Partial Fulfillment of the Requirements for the Ph.D. Degree in Physics

Written by

Zainab Abdulla Mankhi

Supervised by

Prof. Dr. Khalid Ibrahim Riah **Prof. Dr. Ahmed Mehmood Abdul-Lettif**

2023 AD **1445AH**

بِسم الله الرحمن الرحيم

قَالُواْ سُبْحَانَكَ لاَ عِلْمَ لَنَا إِلاَّ مَا عَلَّمْتَنَا إِنَّكَ أَنتَ الْعَلِيمُ الْحَكِيمُ ﴿32﴾

صدق الله العلي العظيم

سورة البقرة

Supervisor Certificate

We certify that the thesis entitled "***Identification of Effective Oral Contrast Agents for Gastrointestinal Magnetic Resonance Imaging***" was prepared under our supervision by (***Zainab Abdulla Mankhi***) at the Science College / Kerbala University as a partial fulfilment of the requirements for the degree of Ph.D. of Science in Physics.

Signature:

Name: Dr. Khalid Ibrahim Riah

Title: Professor

Date: 11/12/2023

Signature: A. M. Abdl

Name: Dr. Ahmed Mehmood Abdul-Lettif

Title: Professor

Date: 11/12/2023

In view of the available recommendations, I forward this thesis for debate by the examining committee.

Signature: M. A. AL-KAABO

Name: Dr. Mohammed Abdulhussain AL-Kaabi

Title: Assistant Professor

Head of Physics Department, College of Science, University of Kerbala

Date: 4 / 1 / 2024

Examination Committee Certification

We certify that we have read this thesis, entitled **"Identification of Effective Oral Contrast Agents for Gastrointestinal Magnetic Resonance Imaging"** and as an examining committee, examined the student **"Zainab Abdulla Mankhi"** on its contents and that in our opinion it is adequate for the partial fulfillment of the requirements for the degree of Ph.D. of Science in Physics.

Signature:
Name: **Dr. Adie Dawood Salman**
Title: Professor
Address: University of Kerbala, College of Science, Department of Physics.
Date: 14/12/2023
(Chairman)

Signature FADHIL
Name: **Dr. Fadhil Khaddam Fuliful**
Title: Professor
Address: University of Kerbala, College of Science, Department of Physics.
Date: 11/12/2023
(Member)

Signature
Name: **Dr. Aedah Zeki Al Kaisy**
Title: Professor
Address: University of Baghdad, College of Medicine
Date: 11/12/2023
(Member)

Signature
Name: **Dr. Ahmed Jumaah Mhawes**
Title: Professor
Address: University of Kufa, College of Medicine.
Date: 11/12/2023
(Member)

Signature:R. A
Name: **Dr. Rajaa A. Madlool**
Title: Professor
Address: University of Kerbala, College of Science, Department of Physics.
Date:11/12/2023
(Member)

Signature:
Name: **Dr. Khalid Ibrahim Raih**
Title: Professor
Address: University of AL-Qadisiyah, College of Medicine, Department of Physiology and Medical Physics
Date: 11/12/2023
(Member & Supervisor)

Signature: A.M.Abd
Name: **Dr. Ahmed Mehmood Abdul-Lettif**
Title: Professor
Address: University of Kerbala, College of Science, Department of Physics.
Date: 11/12/2023
(Member & Supervisor)

Signature: Hassan.J.Jawad
Name: **Dr. Hassan Jameel Jawad AL-Fatlawy**
Title: Professor
Address: **Dean of the College of Science, University of Kerbala**
Date: 4/1/2024

Dedication

To my father's soul,

To my mother's soul,

To my husband, who helped me to achieve my success,

To my daughters (my little angels), who made my life beautiful and blessed,

To my brothers, and sisters, who embraced me with their love and kindness,

To my best friends, who encouraged me.

Zainab A. Mankhi

Acknowledgements

First, thanks to Allah for helping me to complete this dissertation.

Then, I would like to express my sincere appreciation and deep gratitude to my supervisor Dr. Khalid Ibrahim Riah and Dr. Ahmed Mehmood Abdul-Lettif for suggesting the topic of this thesis, guidance, suggestions and continuous encouragement throughout the research.

I would like to express my respect and gratitude to the senior radiologist. Dr. Dhia Mahdey Alghazali (Head Department of Medical Imaging/ Imam Alhasan Almujtaba Teaching Hospital/ Karbala Health Directorate) for his assistance in the qualitative evaluation of the images.

My special thanks go to the staff of the Department of Physics at the College of the Science/University of Kerbala for their assistance and support during the years of my study and research.

Finally, my thanks extend to everyone who helped me in one way or another, and who contributed to make this thesis possible particularly.

Zainab A. Mankhi

Abstract

Magnetic resonance imaging (MRI) has limited use in abdominal imaging since it is difficult to distinguish the alimentary system from normal organs and intra-abdominal lesions. To enhance the vision of inaccessible organs, contrast chemicals are necessary for particular organs, such as gastrointestinal (GI) imaging. Traditionally contrast agents are very expensive, have side effects, and are not always available in Iraqi hospitals. The purpose of this study is to find alternative traditional oral contrast agents that may be employed in MRI of the alimentary tract. These contrast agents must be available, with no or little adverse effects, and non-expensive, modified in water signal intensity during alimentary imaging by MRI to result in high contrast and the best image quality.

The work procedure is summarized by collecting mineral supplements: such as iron, magnesium, potassium, calcium, zinc, sodium, and manganese. Then grinding and dissolving mineral supplements (intake daily dose) in different amounts of distilled water (0.5,1,1.5,2 cup) were performed to obtain solutions with different concentrations (samples). The samples were examined in MRI (1.5 Tesla) using phantoms (tubes) to determine which sample had the lowest level of concentration and best quantitative and qualitative images,

The results of the in vitro study indicate that magnesium, potassium, and sodium supplements have virtually no effect on the water signal intensity in T1-weighted and T2-weighted imaging, whereas calcium supplements raise the water signal intensity on T2-weighted imaging. Manganese and iron supplements raise the water signal intensity on T1-weighted images while decreasing the water signal intensity on T2-weighted imaging, the calcium, manganese, and iron were then evaluated by volunteers.

Thirty healthy individuals underwent MRI scanning both before and after getting a mineral supplement solution. The volunteers were divided into three groups, each with ten volunteers, the first group was given a calcium supplement, the second group was given a manganese supplement, and the third group was given an iron supplement. The MRI of volunteers are evaluated quantitively by measuring the signal intensity, signal-to-noise ratio (SNR), relative signal-to-noise ratios (RSN) and contrast (C), also they are evaluated qualitatively by the radiologist.

From the results of quantitative measurements and qualitative evaluation of MR images, it can be concluded that calcium supplementation can be used as a positive contrast agent on T2-weighted imaging. On the contrary, the manganese and iron supplements act as an excellent positive contrast agent on T1-weighted imaging and a negative contrast agent on T2-weighted imaging.

Contents

List of Tables

List of Figures

List of Symbols and Abbreviations

Symbol	Description
B_o	External magnetic field
I_N	Total angular momentum of the atomic nucleus
$M_Z(t)$	Longitudinal magnetization
$M_{xy}(t)$	Transverse magnetization
f_L	Larmor frequency
ω_o	Angular frequency
ΔE_m	Energy difference between two states
AI	Adequate intake
CAs	Contrast agents
CT	Computed tomography
GD	Gastrointestinal diseases
GI	Gastrointestinal system
h	Planck constant
M	Net magnetic moment
M_0	Magnetic moment
MRA	Magnetic resonance angiography
MRCP	Magnetic resonance cholangiopancreatography
MRI	Magnetic resonance imaging
MRI-GT	Magnetic resonance imaging for the gastrointestinal system
NMR	Nuclear magnetic resonance
RF	Radiofrequency
ROI	Region of interest
RSN	Relative signal-to-noise ratio

S	The spin angular momentum
SCF	The EU Scientific Committee for Food
SD	Standard deviation
SI	Signal intensity
SNR	Signal-to-noise ratio
SPSS	Statistical Package for Social Science Program
t	Time
T1	Spin-lattice relaxation
T2	Spin-spin relaxation
TDS	Total dissolved solids
TE	Echo time
TR	Repetition time
C	Contrast value
k	Boltzmann's constant
γ	gyromagnetic ratio
μ	Magnetic moment of the atomic nucleus
ρ	Spin density

Chapter One

Introduction

1.1 Introduction

Magnetic resonance imaging is the only imaging technique that can recognize damaged tissues or organs apart from healthy ones without the use of ionizing radiation. Strong magnetic fields and radio waves are utilized in this outstanding non-invasive imaging technique to gather quantitative data because of its physical characteristics. Magnetic resonance imaging (*MRI*) has a broad spectrum of clinical uses as an advanced imaging method, including the diagnosis, staging, and management of diseases. On the anatomical, physiological and metabolic information about the human body [1,2]

Imaging is essential for the identification of gastrointestinal diseases (*GD*) since it shows the existence and location of lesions [3]. Endoscopy has been the gold standard for diagnosing (*GD)*, but it is only used for intraluminal testing. For evaluating the gastrointestinal system, cross-sectional non-invasive imaging techniques like computed tomography (*CT*) and magnetic resonance imaging (*MRI*) are superior to endoscopy because they can detect extra-luminal and extra-intestinal disease as well as malignant extra-intestinal complications. MRI imaging characteristics of the gastrointestinal system (*GI*) are indicators of disease activity and response to treatment. When compared to *CT*, *MRI* provides advantages such as the absence of ionizing radiation exposure, reduced abdominal discomfort, and improved soft tissue contrast, which leads to a better evaluation of *GD* and its complications [4,5].

Magnetic resonance imaging is based on the concept of nuclear magnetic resonance (*NMR*), which was developed in the 1940s. As a result, the discussion of MRI starts with an introduction to nuclear magnetic resonance basics [6].

1.2 Physical Principles of *MRI*

Protons and neutrons, the structural components of nuclei, have the quantum mechanical property of spin, which has magnitude and direction. These particles can be seen as little spinning tops. Because of their spin, nuclear particles function like small bar magnets. Inside the nucleus, these small magnets associated with nucleons (protons and neutrons) align to counteract each other's magnetic fields. However, if the nucleon number is odd, the cancellation is incomplete, and the nucleus has a net magnetic moment [7]. As a result, nuclei with an odd number of nucleons act like small magnets. Hydrogen, which has a single proton in its nucleus, possesses a nuclear magnetic moment. The human body is mostly composed of water and other molecules containing hydrogen. As a result, using the magnetic properties of the hydrogen nucleus, MRI images of structures within the body can be obtained most effectively. Our discussion will be limited to hydrogen's nuclear magnetic characteristics [6, 8].

Consider an arbitrary volume of tissue containing hydrogen nuclei (protons) in the absence of an external magnetic field. Every proton has the same magnitude spin vector (or magnetic moment). The spin vectors for the overall collection of protons within the tissue are randomly oriented in all directions; the spin orientations have a continuous distribution. A vector sum of these spin vectors results in a zero total, suggesting that there is no net magnetization in the tissue, as shown in Figure 1.1 [9].

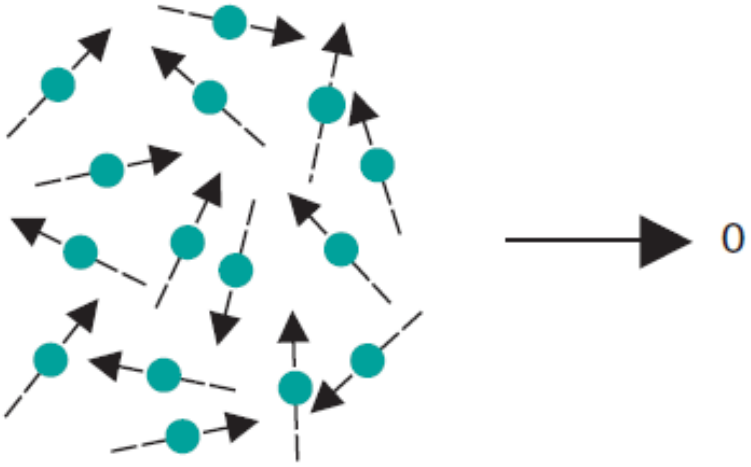

Figure 1.1: In the absence of an external magnetic field, the spins have randomly oriented axes (left side of the figure). The vector sum of these spin vectors is 0 (right side). [9].

When the tissue is placed in a magnetic field (B_o), the individual protons (hydrogen nuclei) begin to rotate perpendicular to the magnetic field, or precess about it. The protons' spin vectors are inclined slightly away from the magnetic field axis, but each axis of precession is parallel to B_o. This precession happens at a consistent pace due to the interaction of the magnetic field with the spinning positive charge of the hydrogen nucleus. The magnetic field and the axis of precession are both defined as being orientated in the z direction of a Cartesian coordinate system. Each proton's motion can be characterized by a set of coordinates that are perpendicular (x and y) and parallel (z) to B_o[10,11]. In the absence of additional interactions, the transverse coordinates are nonzero but fluctuate cyclically with time as the proton precesses, whilst the longitudinal coordinate remains constant, as depicted in Figure (1.2) [9].

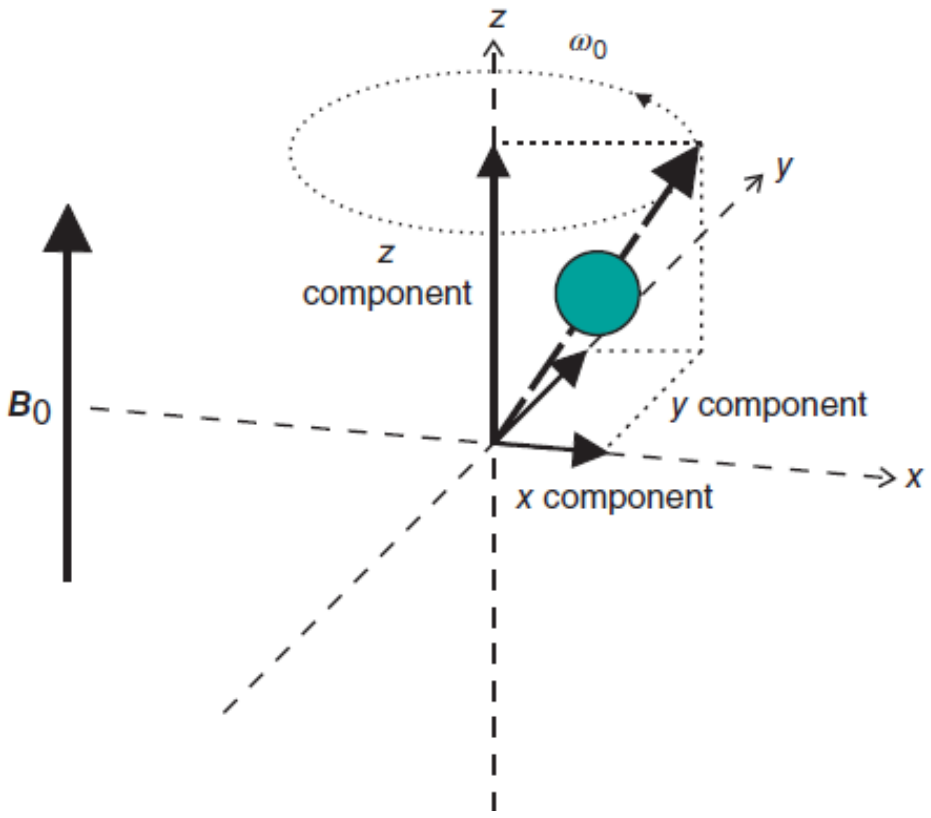

Figure 1.2: In a magnetic field, a proton precesses around the magnetic field. The z component of the spin vector is the component of interest since it does not vary in magnitude or direction as the proton precesses. [9].

Precession frequency is proportional to external magnetic field strength and is represented by the Larmor equation [12]:

$$\omega_o = \gamma B_o \quad \ldots\ldots\ldots (1.1)$$

Where, ω_o is the angular frequency of precession (Larmor frequency), γ is the gyromagnetic ratio in MHz/Tesla. In terms of linear frequency, the Larmor frequency is represented by [11,13]

$$f_L = \frac{\gamma}{2\pi} \cdot B_o \qquad \ldots\ldots\ldots (1.2)$$

γ (the gyromagnetic ratio) is a property of nucleus [14,15]. The gyromagnetic ratio is also defined as the ratio between the magnetic moments (μ) the total angular momentum I_N of the atomic nucleus [16-18].

$$\gamma = \frac{\mu}{I_N} \quad \ldots\ldots\ldots (1.3)$$

A proton or an electron also possesses an intrinsic magnetic moment, in addition to its orbital motion. It is related to and directly proportional to spin angular momentum(s). Therefore, the gyromagnetic ratio for proton or electron is equal to [19]:

$$\gamma = \frac{\mu}{s} \quad \ldots\ldots\ldots (1.4)$$

The volume of tissue containing hydrogen atoms (protons) has no net magnetic moment (*M = 0*) in the absence of a magnetic field. When an external magnetic field is applied, the protons line up either parallel or antiparallel to the magnetic [14]. The assembly of parallel or antiparallel nuclear spins as a whole has a net magnetic moment (***M)*** that acts as a local magnet in the direction of the magnetic field. Because the proton has a fixed orientation with time to the precessional axis, there is a constant, nonzero interaction between the proton and B_o , known as the Zeeman interaction. Instead of a continuous range of values, this interaction leads the z-component of the magnetic moment to be quantized to a finite or discrete number of values. The z-component of the magnetic moment of the proton has just two primary values: parallel B_o and antiparallel B_o. This interaction also results in an energy difference ΔE_m between these two states that are correlated to B_o as depicted in Figure 1.3) [9]. The energy spacing ΔE_m between the parallel and antiparallel alignments equals [14]:

$$\Delta E_m = \frac{\gamma\, hB_o}{2\pi} \qquad \ldots\ldots (1.5)$$

Here *h* is the Planck constant.

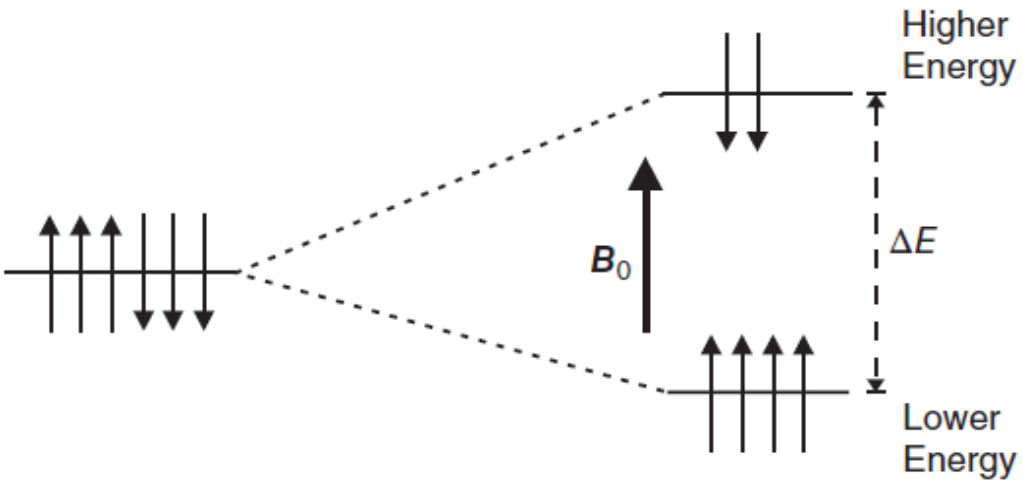

Figure 1.3: Zeeman's diagram. A collection of spins will have z component configurations that are equal in energy in the absence of a magnetic field (left side of the image). The spin-up orientation (parallel to B_0) has less energy and more spins in the presence of a magnetic field (right side) than the higher-energy spin-down configuration. [9, 14].

Spins in parallel (spin up) and antiparallel (spin down) orientations have differing energy as a result of the Zeeman interaction. Spins that are parallel to B_0 have less energy than antiparallel spins. There will be more protons oriented parallel to B_0 than antiparallel, implying that residual polarization of spins created parallel to the magnetic field occurs. The Boltzmann distribution is a distribution function that can predict the precise amount of protons in each energy level. [20,21]:

$$\frac{N_{anti}}{N_{parallel}} = e^{-\frac{\Delta E_m}{kT}} = e^{-\frac{\gamma\, \mathrm{h}\, B_o}{2\,\pi\, kT}} \qquad \ldots\ldots\ldots (1.6)$$

Where k is Boltzmann's constant with a value of $1.38 * 10^{-23}\, J/K$, and T is the temperature measured in Kelvin.

To reverse the alignment of antiparallel spins, energy must be given from an external source. A short radio frequency driving pulse at the Larmor frequency, which is the natural (resonant) frequency of precession, provides the energy necessary to shift the magnetic moment from the direction of the external field [14].

At a higher energy state, the protons' alignment with respect to the static magnetic field B_0 is changed by the radiofrequency field. This is known as excitation. Following a process known as relaxation, the protons that were stimulated by the radiofrequency field will revert to their lower-energy state and reemit RF radiation at the Larmor frequency [2].

1.3 Relaxation

The phenomena of nuclei relaxing occurs when they are stimulated to higher energy levels and then return to their thermodynamically stable states. If an energy level shifts from low to high, energy is absorbed; when the opposite occurs, energy is released [8]. It is a time-dependent process and is characterized by a rate constant known as the relaxation time. Although it is individual protons that absorb the energy, relaxation times are measured for an entire sample of spins and are statistical or average quantities. Relaxation times are measured for grey matter or cerebrospinal fluid as bulk samples rather than for the individual water or fat molecules within the organs. Two relaxation times can be measured, known as Spin-lattice relaxation (*T1*) and Spin-spin relaxation (*T2*). While both times measure the spontaneous energy transfer by an excited proton, they differ in the final disposition of the energy [9].

1.3.1. Spin-Lattice Relaxation (*T1*)

The spin-lattice relaxation time (*T1*) is the time required for the z component of M to return to 63% of its original value after an excitation pulse. The shorter the

relaxation time (*T1*), the more effective the relaxation process. Because the movements between molecules are constrained in solids, the relaxation time (*T1*) values are large. Pulse methods are typically used to measure spin-lattice relaxation [8,22].

The longitudinal relaxation time is another name for the spin-lattice relaxation time. Magnetic moment (M_0) is aligned to B_0 at equilibrium, and energy absorption causes M_0 to spin towards the transverse plane. *T1* describes the process by which protons lose their energy to return to their original orientation. When a 90°-degree pulse is administered to a sample, M_0 rotates and there is no longer any longitudinal magnetism. As the protons release their energy, the longitudinal magnetization will restore over time (Figure 1.4). This magnetization return often follows an exponential growth process, with *T1* describing the rate of growth [9,22].

$$M_Z(t) = M_0\left(1 - e^{-t/T1}\right) \quad \ldots\ldots (1.7)$$

Where $M_Z(t)$ is the longitudinal magnetization as a function of time t and *T1* is the time needed for the recovery of 63% of $M_Z$after a 90-degree pulse (at $t = 0$, $M_Z = 0$, and at $t = T1$, $M_Z = 0.63\ M_0$) [9,23].

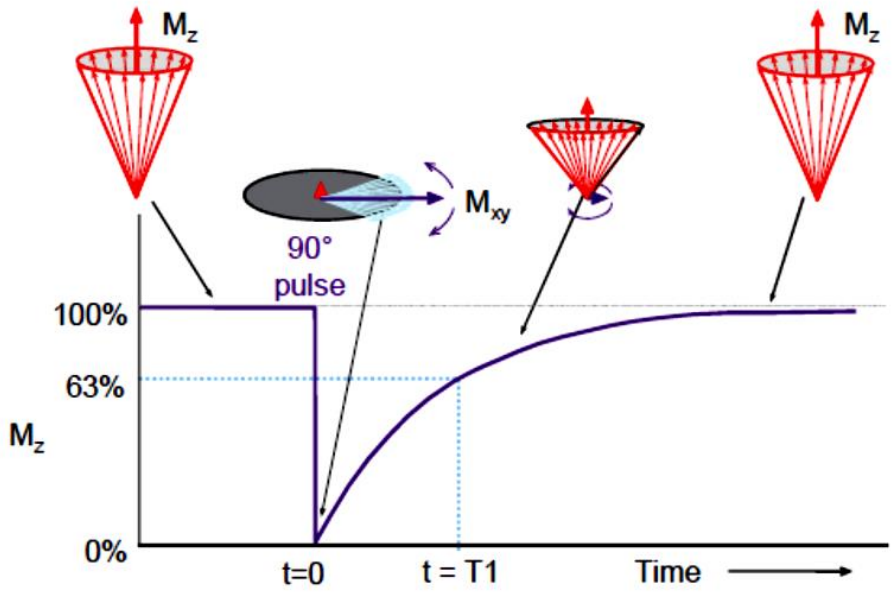

Figure 1.4: Mz is converted from a maximum value at equilibrium to Mz = 0 after a 90-degree pulse. The spin-lattice T1 relaxation characterizes the exponential return of Mz to equilibrium. After a period of time equal to T1[11].

1.3.2. Spin-Spin Relaxation (T2)

Spin-spin relaxation (*T2*) or transverse relaxation time is the amount of time required for the spins to lose coherence with one another. *T2* can be either shorter or equal to *T1* [8,24].

When a radiofrequency *(RF*)pulse is delivered, the magnetization moves into the x-y plane, causing the spins to precess in phase. The net magnetization vector, or transverse magnetization, begins to revolve in the x-y plane around the z-axis immediately after the *RF* pulse is sent. [25].

The *T2* relaxation time is the amount of time that passes between the peak transverse signal (which occurs immediately following a 90-degree *RF* pulse) and 37% of the peak level (1/e) (Fig. 1.5). This can be mathematically represented by the following equation [11,26].

$$M_{xy}(t) = M_0 e^{-t/T2} \quad \ldots\ldots(1.8)$$

Where $M_{xy}(t)$is the transverse magnetic moment at time *t* for a sample that has M_0 transverse magnetization at *t* = 0. When *t =T2*, then $M_{xy}(t) = 0.37\ M_0$[11].

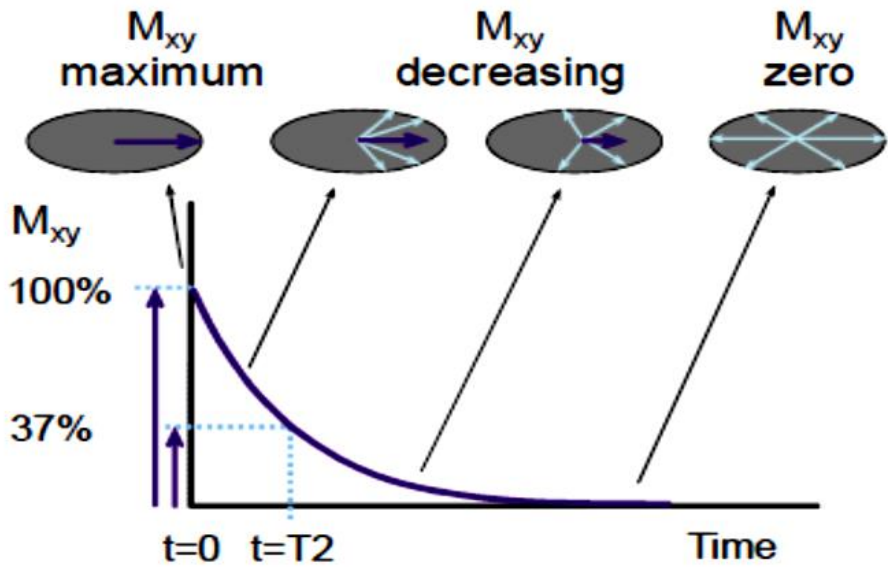

Figure1. 5: Due to inherent spin-spin interactions in tissues, the $M_{xy}(t)$ phase coherence decays exponentially. After a 90-degree pulse, for instance, the exponential decay constant, in order to decay to 37% of its initial transverse magnetization. [11].

1.4 *MRI* Pulse Sequences

In order to produce pictures, radiofrequency pulse sequences and magnetic gradients are programs that are included in *MRI* pulse sequences. There are two types of *MRI* pulse sequences:

- Spin echo (*SE*) sequences.
- Gradient echo (*GRE*) sequences.

In spin echo sequences, a slice-selective 90° excitation pulse is followed by one or more 180° refocusing pulses. The use of excitation pulses with flip angles of

less than 90^{o}, the lack of 180^{o} RF refocusing pulses, and the use of gradient pulses for dephasing and rephrasing set gradient echo sequences apart from other types of echo sequences [2,27].

Gradient echo sequences are generally faster than spin echo sequences and enable for real-time imaging of moving organs such as the heart in the body, the chest (respiratory motion), and the abdomen (peristalsis) [13,28].

1.5 Contrast in *MRI*

The contrast in an *MR* image is produced by *MRI* pulse sequences. There are two parameters in a spin echo sequence that determine the contrast of tissues with the spin density (ρ), the repetition time (*TR*) and the echo time (*TE*) [2,29].

The repetition time is the time interval between two excitation pulses. The echo time (*TE*) is the duration between an excitation pulse and the sampling of the *MR* signal at which the echo maximum occurs [2,30].

In a gradient echo sequence, the flip angle of the excitation pulse, *TE*, and *TR* are factors that determine contrast [2].

1.5.1. *T1* contrast (*T1*-weighted)

Not all of the energy that radio frequency (*RF)* pulse introduced into the system during the excitation is transferred back to the *RF* coil. Some of the energy is wasted and heats the surrounding tissue, known as the lattice. An exponential curve mathematically depicts the time path of the system's return to thermal equilibrium. The longitudinal relaxation time constant *T1* describes this recovery rate [2,31].

The *TR* and *TE* of *T1*-weighted pulse sequences are short. Different body tissues have different *T1* relaxation times. The longitudinal magnetization vector of fat instantly reorganizes with the static magnetic field B_0 after an excitation pulse and appears bright on a *T1*-weighted image. Following a radiofrequency pulse, water realigns its longitudinal magnetization significantly more slowly and looks relatively dark on the *T1*-weighted image. (As shown in Figure 1.6) [2,13]

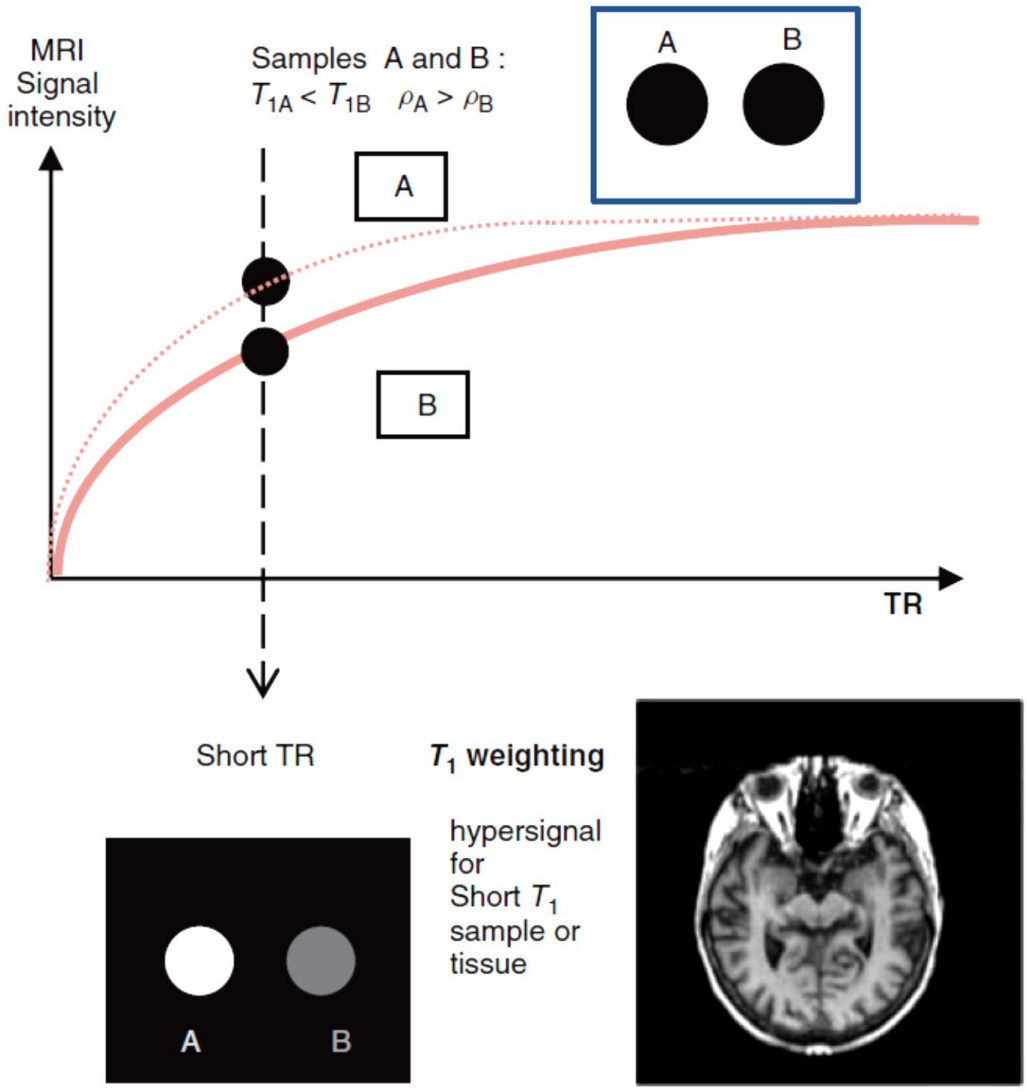

Figure1. 6: T1-Weighted. The intensity of the signal evolves as a function of TR [6].

1.5.2. *T2* contrast (*T2*-weighted)

Random fluctuations in the local magnetic field cause the precession frequency of the nuclear spins in the human body to fluctuate. When nuclear spins exit the phase following an excitation pulse, they lose their initial phase coherence, which is modelled by an exponential decay with the time constant *T2*. *T2* relaxation occurs more rapidly than *T1* relaxation. [2,16]. Long *TR* and long *TE* are used in *T2*-weighted pulse sequences. On *T2*-weighted images, fluid (such as that in the cerebral spaces filled with cerebrospinal fluid (*CSF*)) appears bright, as depicted in Figure 1.7 [6].

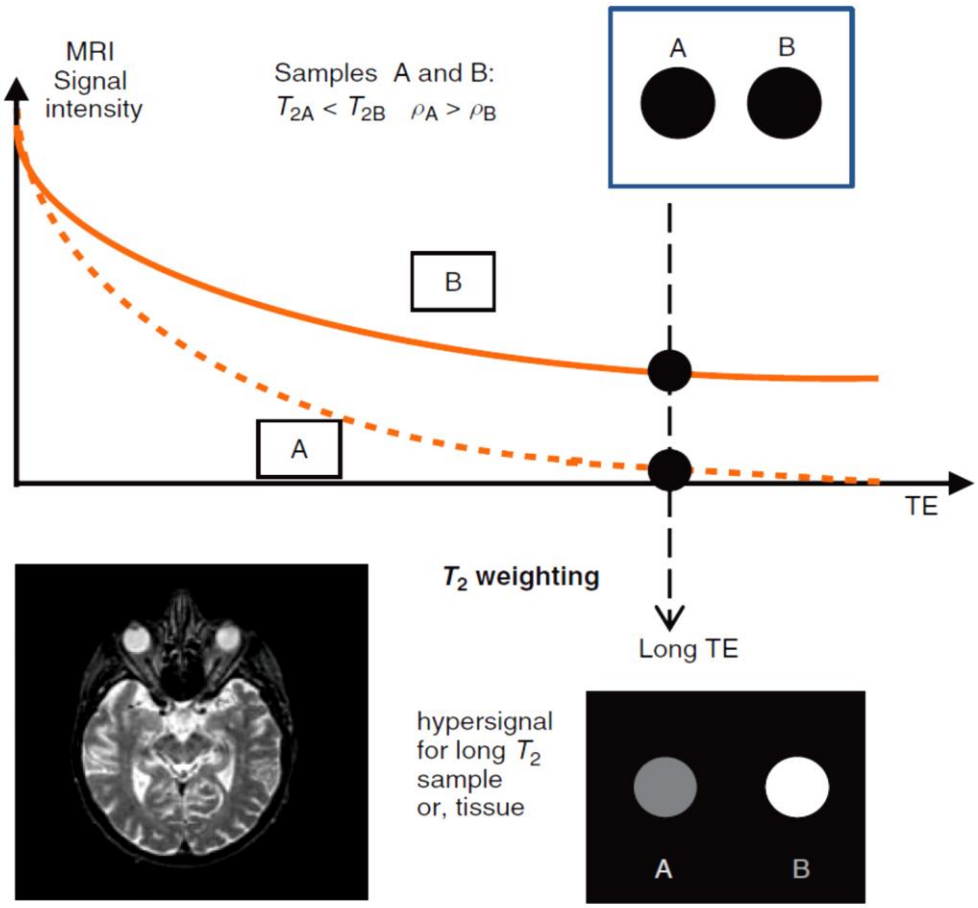

Figure1.7: T2-Weighted. The intensity of the signal evolves as a function of TE [6].

1.5.3. Proton density contrast (*Pd*-weighted)

In order to reduce the impacts of *T1* and *T2*, the scan settings are controlled to create proton density-weighted images, which have strong dependence on the density of hydrogen protons in the imaging contrast. Proton density-weighted sequences have a short *TE* a and long *TR* [30,32].

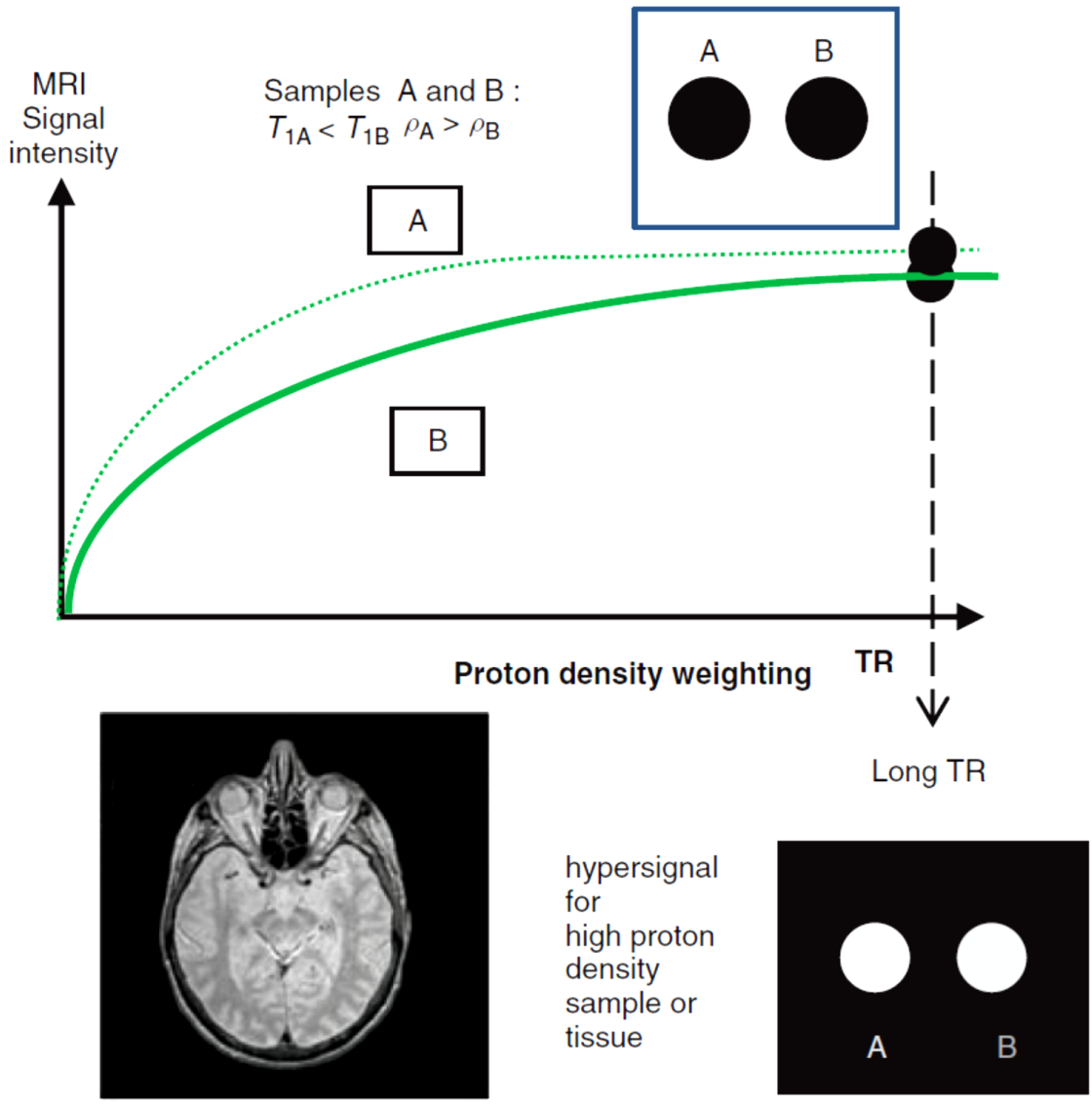

Figure 1. 8: Proton density Pd-weighted image. The intensity of the signal evolves as a function of TR [6].

1.6 *MRI* Contrast Agents

Contrast agents are required in some organs, such as gastrointestinal (*GI*) imaging, to improve the visualization of inaccessible organs. Depending on the target tissue, *MRI* contrast agents can be given orally or intravenously [13].

1.6.1. The intravenous contrast agents

Most scans, including extracellular mediators and blood pool agent imaging, musculoskeletal and neurological *MRI*, routinely use intravenous delivery of contrast agents [1]. The ionic compounds of a new generation of imaging agents were Gd-DTPA (Magnevist) and Gd-DOTA (Dotarem, Artirem). These complexes have low toxicity as well as strong thermodynamic and kinetic stability. These two compounds are high osmolar contrast agents (*CAs*), although being well tolerated. As a result, two non-ionic gadolinium chelates are formed [10].

1.6.2. The oral contrast agents

Oral contrast agents are typically administered for *GI* and hepatobiliary examinations [1]. When utilizing MRI for gastrointestinal imaging, it has been difficult to distinguish the gastrointestinal (*GI*) tract from intra-abdominal masses and normal organs. For assistance with this problem, various oral items have been used as contrast agents [16].

The first gadolinium-based contrast agent (*CA*) for magnetic resonance imaging (*MRI*) was constructed in the late 1980s. These solutions have been used as oral contrast agents [33,34], with the gadolinium-based solution (Gd) acting as a positive contrast agent and the barium dilute (2%) (which is diamagnetic) acting as negative contrast media on *T2* weighted [35].

Contrast agents for gastrointestinal *MRI* vary and might be either positive or negative. *GI* contrast agents are classified as either positive (bright on *MRI*) or negative (black on *MRI*). There are several gastrointestinal *MRI* contrast media available, although they are rarely employed. They are categorized as either positive or negative enhancers based on whether they raise or reduce the signal from the *GI* lumen. They are also categorized according to their magnetic properties [36,37]:

a. Paramagnetic Agents:

Atoms or molecules that have a magnetic moment, such as unpaired nucleons in their atomic nucleus or unpaired electron orbits in their outer electron shells (resulting from individual spins), make up paramagnetic substances. A local increase in the magnetic field occurs when a material with these characteristics is subjected to an external magnetic field because the bulk of the magnetic moments align with the direction of the magnetic field [19].

b. Diamagnetic Agents:

Diamagnetic materials represent the vast majority of all substances. Diamagnetic materials produce a relatively weak overall magnetization in the opposite direction (-z) when exposed to an external magnetic field, mostly because the majority of electrons move in counterclockwise orbits [38,19].

c. Superparamagnetic Agents:

Ferromagnetic materials are made up of atoms whose unpaired electron spins have a strong exchange coupling interaction (solid-state). These materials become permanent magnets when the external magnetic field gets removed. The most common example is iron (*Fe*) [38].

1.6.3. Oral contrast agents side effect

MRI oral contrast media, like any medicine, can cause moderate allergic reactions, nausea, flushing, headache, rash, and nephrogenic systemic fibrosis, which is one of the most serious side effects of the gadolinium-based solution contrast agent [20,37]. Barium sulfate is used in traditional radiographic gastrointestinal examinations; however, some can leak into the respiratory tract. High density barium has been used as an oral contrast agent for *MR* imaging of the gastrointestinal tract, but this method frequently requires substantial amounts of contrast to be taken, which is not recommended for small children or neonates [39].

1.7 Characteristics of MR Image

The influence of MRI contrast agents on the proton relaxation process alters MRI signal intensity, increasing contrast and informative value [40]. Images were evaluated qualitatively and quantitatively by measuring the anatomical signal-to-noise ratio (SNR), relative signal-to-noise ratio (*RSN*), and contrast value.

The signal intensity (*SI*)that determines the contrast of tissue in MR images with the spin density ρ, the repetition time (*TR*), and the echo time (*TE*) [2]

$$SI = \rho.\left(1 - e^{\frac{-TR}{T1}}\right) * e^{\frac{-TE}{T2}} \quad \ldots\ldots\ldots (1.9)$$

The signal-to-noise ratio (*SNR*) is referred to as the quotient between the signal intensity (*SI*) collected in the region of interest (*ROI*) and the standard deviation of the signal intensity in an area outside the object being scanned [13]. *SNR* is calculated using the formula that is shown below. [35,41].

$$SNR = \frac{mean\ (SI) of\ solution - \ mean\ (SI) of\ background}{standard\ deviation (SD) of\ background} \quad \ldots\ldots\ldots (1.10)$$

The relative signal-to-noise ratio (*RSN*) is calculated using the following formula [35]:

$$RSN = \frac{SNR\ of\ solution}{SNR\ of\ water} \quad \ldots\ldots\ldots\ldots (1.11)$$

Contrast refers to the difference in signals between two adjacent locations, such as those between tissues or those between a contrast agent and the tissues around it.

$$C = SI_A - SI_B \quad \ldots\ldots (1.12)$$

$SI_A\ and\ SI_B$ are signals of two nearby tissues or of a contrast agent and tissues around it [16].

1.8 MRI Safety

Since MRI does not use ionizing radiation, the general public thinks it to be a highly safe method. However, safety is sometimes an afterthought, especially when it comes to operational operations and training of personnel who operate in the region and around the magnet. For MR, there is a great deal of significant bioeffects and safety concerns to take into account. Strong magnetic fields, radio frequency energy, magnetic gradient fields that change over time, enclosed imaging devices (claustrophobia), and noisy operation (gradient coil activation and deactivation, which produces acoustic noise) are some of these bioeffects and safety concerns. Patients who have heart valves, aneurysm clips, implants, prostheses, or other devices should be informed that these devices have significant torque and that placing them in a magnetic field could have substantial negative effects [11,42].

Cardiac pacemakers are not suitable for *MRI* because they contain a number of sensitive electrical components, the function of which may be affected during the scan. Pacemaker electrodes are efficient antennas for receiving *RF* radiation, which can cause arrhythmia. Furthermore, the electrodes may heat up, resulting in burns or thrombosis of blood vessels. This also applies to the vast majority of patients who have transient pacemakers. Patients should not get *MRI* follow-up following coronary stenting until at least six weeks have passed [13]. In patients who have internal defibrillators or left ventricular assist devices, *MRI* scanning is not recommended. Neurostimulators and cochlear implants are also contraindicated [9, 13].

Patients with imbedded metal fragments or bullets should be treated with caution as well. The risk presented by these foreign entities is often defined by their anatomic position as well as whether or not they are ferromagnetic. If ferromagnetic objects are placed in a sensitive region, such as the eye, they might hurt the optic nerve if they change during the scan. Under rapidly changing gradient fields, nonmetallic implant materials can also cause considerable heating. The distortions on the acquired images, as well as the likelihood of misdiagnosis, are important factors to consider [9,11].

Patients with large tattoos may also experience issues, which can occasionally result in burns. So, it should be removed prior to the scan [13].

Chapter Two

Literature Review

2.1 Literature Review

There are many studies aimed at replacing traditional oral contrast agents with safe and inexpensive materials, they are summarized below:

- Riordan *et al.* [43] (2004) demonstrated that pineapple juice can be utilized as a negative oral contrast agent to improve cholangiopancreatography (*MRCP*) image quality. This impact is most likely due to the paramagnetic effect of pineapple juice's relatively high manganese content, which reduces the *T2* relaxation time for the fluid in the stomach and duodenum. This study was conducted on phantoms and adults.
- Espinosa *et al.* [44] (2006) used phantoms to study six fruits and discovered that blackberry pulp should be evaluated as a potential oral contrast agent when imaging of the gastric region of the *GI* tract is conducted in *MRI* by healthy volunteers. Because blackberry enhancement is more effective in gastrointestinal problems. The results demonstrated that *T2*-weighted images exhibited negative behavior whereas *T1*-weighted images exhibited positive behavior.
- Cordova-Fraga *et al.* [45] (2012) studied the physical and chemical properties of pulp from Achras sapota L. (common medlar). It was studied using phantoms in vitro and Gastric MRI in vivo. The results revealed a negative behavior on *T1*-weighted images and a positive behavior on *T2*-weighted images.
- Shi *et al.* [46] (2012) demonstrated that 2.5% magnesium sulfate ($MgSO_4$) can reduce water absorption in the small bowel and completely fill the enteric cavity, enhancing the contrast between the intestinal wall and lumen and allowing *MRI* examination of the small bowel. Twenty participants were scanned after drinking 2.5% ($MgSO_4$). Intestinal problems can be detected using an MRI with 2.5%

($MgSO_4$). As a result, 2.5% ($MgSO_4$) solution is an excellent oral contrast media (*CM)* for small bowel *MRI*.

- Elsayed *et al.* [47] (2015) investigated natural oral contrast agents in intestinal magnetic resonance imaging. Fourteen healthy individuals took part in the study. Each volunteer underwent three *MRI* exams on different days using three different oral contrast materials: water, milk, and pineapple juice. According to the study's results, pineapple juice has the highest ability of intestinal distention and good images within considerable image.
- Faletti *et al.* [48] (2018) compared in vitro pineapple juice to a solution of concentrated pineapple juice with a paramagnetic contrast agent to determine the feasibility of using the solution of concentrated pineapple juice in vivo for esophageal visualization during magnetic resonance angiography (*MRA*) prior to radiofrequency catheter ablation for atrial fibrillation. The results showed that, following suitable concentration procedure and the inclusion of modified potato starch, pineapple juice is as hyperintense as the *MRI* diluted contrast solution, allowing for practical and safe esophagus vision during *MRA*.
- Hapsari *et al.* [49] (2019) demonstrated the effect of pineapple juice and black tea, both natural sources of negative oral contrast, in the visibility of the pancreatobiliary system during an *MRCP* examination. The results demonstrated that black tea was more successful than pineapple juice in producing superior image results on *MRCP* examinations without the use of oral contrast. The metal content of negative oral contrast might result in magnetic susceptibility, which is characterized by shortening during *T2* relaxation.
- Isnoviasih *et al.* [50] (2019) used superparamagnetic iron supplement solutions as a replacement for negative contrast media. This study compared the variations in stomach SNR values on MRCP before and after administering an iron

supplement solution as a substitute for negative oral contrast media. The study's participants used a pre-contrast, post-contrast scanning technique to scan 10 healthy adults. The signal value is used to determine the SNR based on the picture result, and a subsequent examination is then carried out. Images from the test results demonstrated that iron supplement solutions might be employed as a negative oral contrast medium for MRCP testing.

- Mohabir *et al.* [51] (2020) employed a commercially available pineapple juice solution as a negative oral contrast agent for *MRCP*. The study included fifty adult patients. The results of this investigation demonstrated that the local pineapple juice preparation employed in this study is an excellent, inexpensive, and natural negative oral contrast agent for enhancing *MRCP* images.
- Pinho *et al.* [52] (2020) conducted research to evaluate the two contrast agents used in *MRCP* and the quality of the images using the image J® program. We picked a variety of natural juices and pulps, including açai powder and liquid as well as a blend. At Clinical Hospital, the subjects (thirty-three men and thity-one women) were selected to take part in the study. As it should be in the clinic for a high-quality image in *MRCP*, natural contrast (açai) was discovered to be capable of eliminating signal from the stomach and duodenum as well as boosting the signal to the common bile duct.
- Utami *et al.* [53] (2021) carried out the first experimental investigation using jasmine tea as an oral contrast agent with the goal of evaluating how effective it is in enhancing the *MRCP* quality of images. Healthy participants and phantoms were used to test this investigation. Following testing of several tea phantom kinds, the signal-to-noise ratio (*SNR*) value was determined and the manganese concentration was examined. Before and after the administration of jasmine tea, fifteen healthy volunteers underwent *2D T2 HASTE* thick-slab *MRCP* scanning with a range of three minutes, six minutes, and nine minutes of scanning duration.

The findings of this study demonstrated that jasmine tea may be utilized as a substitute natural negative oral contrast agent, increase the quality of the MRCP picture, and lessen the strength of gastrointestinal signals.

- Vesna *et al.* [54] (2022) employed pineapple juice (*PJ*) instead of commercially available negative contrast agents during *MRCP* because the pancreaticobiliary ducts might be obscured by the high-intensity signal from the stomach and duodenum. The study included 10 *MRCP*-examined patients and 10 healthy subjects. According to the findings of this study, pineapple juice is an effective, inexpensive, and natural negative oral contrast agent that provides effective signal suppression in the *GI* tract on *MRCP*, with no significant difference in image quality between fifteen and thirty minutes after consuming the juice.
- Suner *et al.* [55] (2023) conducted an in vitro study on Chondroitin sulfate (*CS*) that was physically crosslinked with *Fe (III)*. The contrast enhancement abilities of aqueous *CS-Fe* ion particle suspensions in magnetic resonance imaging (*MRI*) were determined by obtaining *T1*- and T2-weighted *MR* images using a 0.5 Tesla *MRI* scanner and calculating the water proton relaxivities. As a result, particles have the potential to enhance image contrast in *MR* imaging on *T1*-weighted while also acting as negative contrast agents on *T2*-weighted images.
- Islam *et al.* [56] (2023) conducted a study on Manganese Complex of 1,4,7-Triazacyclononane-1,4,7-Triacetic Acid (*NOTA*) as a Hepatobiliary *MRI* Contrast Agent, *Mn-NOTA-NP* demonstrates a r1-relaxivity of 3.57 mM^{-1} s^{-1} in water and 9.01 mM^{-1} s^{-1} in saline containing human serum albumin at 3 Tesla. The results of this study exhibited that Mn-*NOTA-NP* can be a beneficial alternative to Gd^{3+}-based hepatobiliary agents because it shows the best properties as a liver-specific MRI agent.

2.2 The aim of Present work

This research aims to find alternative traditionally oral contrast agents that can be used in *MR* imaging of the gastrointestinal system, these contrast agents must be:

- Available.
- With the minimum or no adverse effects.
- the low cost.
- Change the signal intensity of water during gastrointestinal imaging by MRI.
- Give high contrast and the best imaging quality.

Mineral supplements (such as calcium, zinc, iron, potassium, magnesium, sodium, and manganese) have been proposed as alternate contrast agents in this study because the preceding conditions have been satisfied and affect the magnetic field.

Chapter Three

Materials and Methods

3.1 Introduction

In this chapter, materials used as alternatives to traditional contrast agents are presented. Mineral supplements have been suggested as alternative contrast agents in the MRI because they are available in pharmacies, are non-expensive, have no or minimum side effects, and affect the magnetic field. After that, the procedure for preparing supplement solutions and the MR imaging protocol will be explained.

3.2 Mineral Supplements

In this research, we have used mineral supplements that are affected by the magnetic field of the type paramagnetic and superparamagnetic types. Mineral supplements are available in local pharmacies, such as calcium, zinc, iron, potassium, magnesium, sodium, and manganese.

A summary of the characteristics of each mineral supplement will be provided in the following.

3.2.1 Calcium

Calcium (*Ca*) is an element in the Periodic Table of Elements Group II (the third period). It has a valence of two [57], an atomic weight of 40.08, and an atomic number of twenty. The element calcium possesses paramagnetic characteristics [58].

Calcium is available as dietary supplements in a number of forms, such as calcium chelates and calcium carbonate. Calcium carbonate contains the highest concentration of elemental calcium. However, it is less soluble and thus less accessible than calcium chelates. Calcium carbonate is found in antacid medications (with a daily maximum intake of 4000 mg of calcium) [59,60]. This

argument underpins the 1000mg daily consumption recommendation for adults [61,62].

Toxic consequences of high calcium consumption have only been described when calcium is administered in the carbonate form at very high doses; this toxicity is induced by the alkali as well as the calcium and is caused by calcium salt precipitation in renal tissue (milk-alkali syndrome). In practice, however, a calcium intake limit of 3g (75mmol) is recommended [61,63]. Renal calcium excretion occurs through the glomerular filtration process (adults excrete around eight to ten grams of calcium each day) [57,64].

3.2.2 Zinc

Zinc is a group IIB of the Periodic Table of Elements with an atomic weight of 65.37. Zinc exists as Zn^{2+} in biological systems and is found in all tissues and fluids throughout the body [57]. Zinc possesses diamagnetic properties [58].

In the traditional sense, the body has no zinc reserves. Zinc is liberated and may be reutilized to some extent during bone resorption and tissue catabolism [61, 65]. Urinary zinc excretion ranges from 300 to 700 g/day [57].

Under European legislation, the zinc salts acetate, citrate, chloride, gluconate, oxide, lactate, carbonate, and sulphate are listed in the list of chemicals that can be employed in the preparation of foods for specified nutritional applications and in mineral supplements [57].

Many approved medications contain zinc, either by itself or in combination with other chemicals, and they are used to treat and prevent deficiency. The acute toxic effects of zinc occur at levels of around 200 mg or greater, while the maximum daily intake of medications available is through a pharmacist is 150 mg [59, 63].

After consuming 4–8g (60–120 mmol) of zinc, symptoms such as nausea, vomiting, diarrhea, fever, and fatigue have been noted. However, prolonged intakes of zinc above what is necessary may interfere with the metabolism of other trace metals. High zinc doses appear to be particularly susceptible to copper [61].

3.2.3 Iron

The atomic mass of iron metal is 55.8. One of its two oxidation states is present in biological systems, and the redox interconversions of the ferric (Fe^{3+}) and ferrous (Fe^{2+}) forms are crucial to the mineral's biological characteristics. Oxygen carriers like myoglobin and hemoglobin require iron as a necessary component [57,59,66]. Iron is a super paramagnetic property [58].

Ferrous salts (chloride, fumarate, gluconate, glycerophosphate, succinate, sulphate) are more easily absorbed than ferric salts. The most prevalent are ferrous sulphate and succinate [59].

Iron is not actively eliminated from the body through the kidneys or the intestines. Only cells from the skin and the interior surfaces of the body (the intestines and urinary tract) lose iron. Iron is reversibly stored in the liver as ferritin and haemosiderin, and it is distributed throughout the body through protein transferrin [61]. Supplemental iron levels of 50-220 mg/day and higher have been caused by vomiting, nausea, and pain in the abdomen [63, 67].

3.2.4 Potassium

Potassium is an alkaline metallic element. It is never found in its elemental form in nature and is always found in conjunction with other chemicals, most often as chloride salt (KCl) [59], potassium has paramagnetic properties [58].

Potassium chloride is commonly used in dietary supplements, although several other forms, such as potassium citrate, phosphate, aspartate, bicarbonate, and gluconate, are also utilized [67].

The kidneys are the main potassium excretory pathway. It is secreted by the renal tubules in exchange for sodium from the glomerular filtrate (ion-exchanging process). Sweat and feces excretion are insignificant [59].

However, a few case studies have shown that adults who appear to be in good health can experience negative effects on heart function from supplemented potassium levels of 5-7 g/day. In addition, people who are healthy using several types of potassium supplements at doses ranging from roughly 1-5 grams of potassium per day have reported experiencing gastrointestinal symptoms (discomfort, mucosal sores, and occasionally ulceration) [57, 68]. The serving of dietary supplements contains no more than 99 mg of potassium [67].

3.2.5 Magnesium

Magnesium (*Mg*) belongs to the Periodic Table of Elements Group II, which also contains two other medically important elements: calcium and magnesium. The atomic weight of Mg is 24.312, the atomic number is 12, and the valency is two [57,59]. Magnesium is a paramagnetic metal [58].

Mg is commonly bound or chelated in food derived from plant and animal sources, such as phytic acid, phosphates, and chlorophylls, or it is integrated into biological apatite (skeleton) [57, 69]. Mg salts (such as chloride, sulfate, phosphate, carbonate, and citrate) dissociate in aqueous solutions based on concentration, temperature, and pH [57]. The current upper limit for magnesium in a dietary

supplement is 600 mg per day dose. The daily minimum for magnesium is 75 mg [70].

Magnesium is mostly eliminated in the urine [59]. Human kidneys are capable of swiftly excreting significant amounts of magnesium that have been ingested or injected. Even after massive doses, serum levels often remain within the normal and safe range. Subjects with normal kidneys can excrete 40 to 60 g of magnesium per day as a continuous infusion without having any deleterious effects.

Magnesium-containing medications, typically antacids and cathartics, are taken more than 15 g per day on a chronic basis, and blood levels can rise. Moderate elevations in plasma magnesium levels might cause nausea, vomiting, and hypotension [63].

3.2.6 Sodium

Sodium (Na^+) is a 22.99 atomic mass alkali metal. Sodium is a solid metal at normal temperatures and pressures; it is extremely reactive in both water and air and is not found naturally in its elemental form [57]. Sodium has paramagnetic properties [58].

The major component of table salt is sodium chloride (*NaCl*). A gram of sodium chloride contains 0.4 grams of sodium and 0.6 grams of chloride. Sodium-containing food additives that can be added to both foods and supplements include riboflavin, sodium iodate, sodium carbonate, sodium citrate, sodium lactate, sodium salts of orthophosphoric acid, sodium selenite, sodium fluoride, sodium borate, sodium iodide, sodium bicarbonate, sodium gluconate, sodium hydroxide, sodium selenate, sodium hydrogen selenite, and sodium molybdate [71].

All adults were given an adequate intake (*AI*) of 1.5 g/day. Adults should limit their sodium intake to less than 2.3 g per day, according to the 2015-2020 Dietary

Guidelines for Americans [71,72]. However, consuming too much sodium can result in high blood pressure, heart disease, stroke, and coronary heart disease [73].

Sodium excretion by the gastrointestinal and respiratory tracts is insignificant under normal conditions, and sodium is largely excreted by the kidneys [74].

3.2.7 Manganese

A typical metallic element called manganese may exist in a variety of oxidation states. The most significant Mn ions in life are Mn^{2+} and Mn^{3+} [59]. There are several different oxidation states of manganese, with Mn (II) being the most prevalent in biological systems [57]. Manganese possesses paramagnetic properties [58].

The EU Scientific Committee for Food (*SCF*) determined that a safe and appropriate consumption was 1-10 mg/person/day [57,59]. Manganese is primarily eliminated in the feces, primarily through biliary excretion, but some direct secretion occurs. Manganese is eliminated in small quantities in the urine. Human volunteers in supplementation experiments with 15 or 9 mg manganese/day for 124 days and “many months” respectively had no deleterious effects. There is some evidence that drinking water having higher levels of manganese may have less severe neurotoxic effects at lower levels of exposure. Muscle pain, weariness, tremor, memory issues, and reduced reflexes are among the symptoms mentioned [59,75].

Manganese is found in many various forms in dietary supplements, including amino acidchelates (e.g., manganese bisglycinate chelate, manganese glycinate chelate, and manganese aspartate). Manganese gluconate, manganese picolinate, manganese sulfate, manganese citrate, and manganese chloride are some more types [76].

3.3 Devices

There are many devices used in this study as the following:

3.3.1. Millers

The millers were used to grind the mineral supplement tablet to increase and accelerate its solubility in distilled water (Figure 3.1).

3.3.2. Digital balance

Digital balance is used to measure tablet weight before and after grinding. Manufacturer country: China (Figure 3.1).

3.3.3. Thermometer

The thermometer is utilized to measure the temperature of samples before scanning in MRI. Manufacturer country: China (Figure 3.1).

3.3.4. Total Dissolved Solids (*TDS*) meter

TDS is an abbreviation for Total Dissolved Solids meter, which represents a measure of the total charged mineral content of water before and after dissolving a mineral supplement tablet in distilled water. The total amount of dissolved solids (ppm) is commonly displayed by *TDS* meters. Manufacturer country: China (Figure 2.1).

3.3.5. *MRI* scan

Images of this research were obtained using *MRI* -1.5Tesla (Siemens-Germany). The solutions were tested in MRI by tubes and healthy volunteers.

a-Miller

b-Digital balance

c-Thermometer

d-TDS meter

e- MRI scan

Figure 3.1: Devices used in the research

3.4 Preparing Samples(solutions)

Grinding and dissolving mineral supplements (intake daily dose) in different amounts of distilled water (0.5,1,1.5, and 2 standard cups (1 cup=240ml) were performed to obtain solutions (samples). For example, two calcium supplement tablets (containing 1000 mg of calcium carbonate$CaCO_3$) were dissolved in each (0.5,1,1.5, and 2 standard cups) of distilled water (*TDS*=0ppm), in another way:

- 1000 mg of calcium carbonate+0.5 standard cup of distilled water represents sample1of calcium solution.
- 1000 mg of calcium carbonate+1 standard cup of distilled water represents sample 2 of calcium solution.
- 1000 mg of calcium carbonate+1.5 standard cup of distilled water represents sample 3 of calcium solution.
- 1000 mg of calcium carbonate+2 standard cup of distilled water represents sample 4 of calcium solution.

The four samples and distilled water were examined using test tubes to determine which sample had the lowest concentration and the best quantitative

image. This sample was then examined by a healthy volunteer.

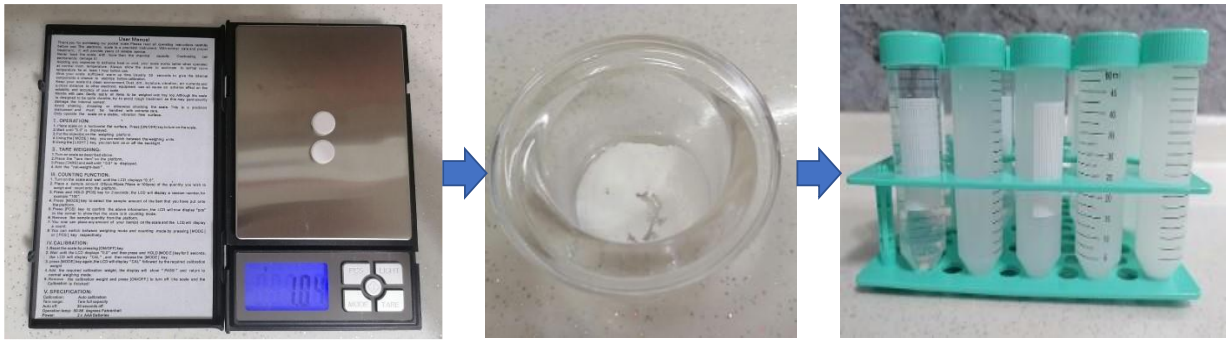

Figure 3.2: procedure of preparing samples(solutions).

The dissolved amounts of the investigated mineral supplement are shown in Table 3.1.

Table 3.1: The doses of mineral supplements used in this research and compared with reference daily dose.

Mineral supplements	The chemical composition of the supplement	the dose used (mg)	Reference daily dose (mg)
Calcium	Calcium carbonate	1000	1000-4000
Zinc	Zinc sulfate	125	40-150
Iron	Ferrous sulfate	200	50-220
potassium	Potassium gluconate	99	1000
Magnesium	Magnesium citrate	500	75-600
Sodium	Sodium bicarbonate	500	1500-2300
Manganese	Manganese citrate	4	1-10

3.5 Phantom Study

An imaging phantom or "phantom" is a scientific device that is often used in the biomedical research community. A phantom is a specially designed object that is utilized as a "stand-in" for human tissue and can be scanned or imaged to evaluate, analyze, and fine-tune the performance of an imaging device.

Phantom experiments of varying concentrations for different mineral supplements were performed on 35 phantoms (tubes), including 7 phantoms of distilled water (control), followed by MRI-GI scanning. The signals of the image's results were measured using a region of interest *(ROI*) signal (area 300 mm^2).

The sample with the lowest concentration and the best quantitative image was then evaluated by healthy individuals.

Figure 3.3: Phantom experiments procedure.

3.6 Volunteers Study

This is a quasi-experimental study with a pre-and post-test design. The subjects of this study were 30 healthy volunteers who received an *MRI-GI* examination with standard preparation of fasting 8 hours before the procedure. The treatment consists

of an oral mineral supplement solution that is scanned 3 minutes after oral supplement solution administration [53]. The individuals chosen were healthy, had no history of claustrophobia, had no metal implants, and were not pregnant.

3.7 Quantitative Analysis of MR Images

The image quality of the magnetic resonance equipment was assessed using the signal intensity (*SI*), signal-to-noise ratio (*SNR*), relative signal-to-noise ratios (*RSN*), and contrast (*C*) of each MR image. Drawing a 300 mm^2 region of interest (*ROI*) in the area of the alimentary tract for each participant allowed us to calculate the signal intensities.

The *SPSS* (Statistical Package for Social Science) program, version 22.0, was used to analyze the data. The quantitative values were estimated using the mean and standard deviation (*SD*). The t-test for quantitative data was used in two-set comparison to examine quality differences. P-values < 0.05 for both sides were considered statistically significant.

The P value is defined as the chance of receiving a result equal to or more extreme than what was seen under the premise of no impact or difference (null hypothesis). The P stands for probability, and it indicates the likelihood that any observed difference between groups is attributable to chance. Because P is a probability, it can have any value between 0 and 1. Values near 0 indicate that the observed difference is unlikely to be attributable to chance, whereas values close to 1 imply that there is no difference between the groups other than through chance [77].

Correlation is a statistical measure (a number) that represents the magnitude and direction of an association between two variables.

The Pearson correlation technique is the most often used approach for numerical variables; it provides a number between 1 and -1, where 0 indicates no connection, 1 indicates an entire positive correlation, and -1 indicates a total negative correlation [78,79].

3.8 Qualitative Analysis of *MR I*mages

The subjective image quality was evaluated separately by the radiologist, who has 11 years of expertise in *MR* Imaging. A four-point Likert scale has been used to rate subjective image quality while taking contrast into account:

1 =poor; 2= sufficient; 3 = good; 4 = excellent.

A Likert scale is a type of rating system used to quantitatively evaluate opinions, beliefs, attitudes, or actions. It consists of four or more questions [80,81].

3.9 Protocol of *MR I*maging

The 1.5Tesla-*MRI* machine (Siemens) was used to create the images for the tests, and the imaging conditions are as follows:

- ***T1*-weighted**

- two-dimensional type.
- gradient echo sequences, the flip angle is 65 degrees.
- repetition time of image *TR* =6.16 msec.
- echo time of image *TE*= 2.15 msec.

- ***T2*-weighted:**

- two-dimensional type
- turbo spin echo sequence, 140-degree flip angle.
- repetition time *TR*=2400 msec.
- echo time of image *TE*= 689 msec.

Both in vitro and in vivo experiments utilized the same *T1* and *T2* weighted. By constructing a region of interest (*ROI*) with an area of 300 mm^2, the average signal intensity on each phantom and the stomach region was computed.

3.10 Research Sitting

Before taking part in the study, all individuals provided their informed permission. The study was carried out in compliance with the Helsinki Declaration, and the protocol was approved by the Ethics Committee of the Medical Research Committee, Training, and Human Development Center, Karbala Health Department, Iraqi Ministry of Health. When the search number (2022020/ Karbala) was on the date 2022/2/2

The MRI department at the Imam Zain El Abidine Hospital in Karbala, Iraq, was the place of conduct of this experimental work.

3.11 Procedure of the work

1. Collect mineral supplements: such as iron, magnesium, potassium, calcium, zinc, sodium, and manganese.
2. Preparing samples: Grinding &dissolving mineral supplements (intake daily dose) in different amounts of distilled water (0.5,1,1.5, and 2 standard cups) to obtain solutions (samples).
3. Imaging samples by *MRI.*

4. Analyzing vitro data: The best sample will be tested by volunteers.
5. Imaging volunteers by *MRI.*
6. Analyzing vivo data.

   The procedure can be summarized in the following chart

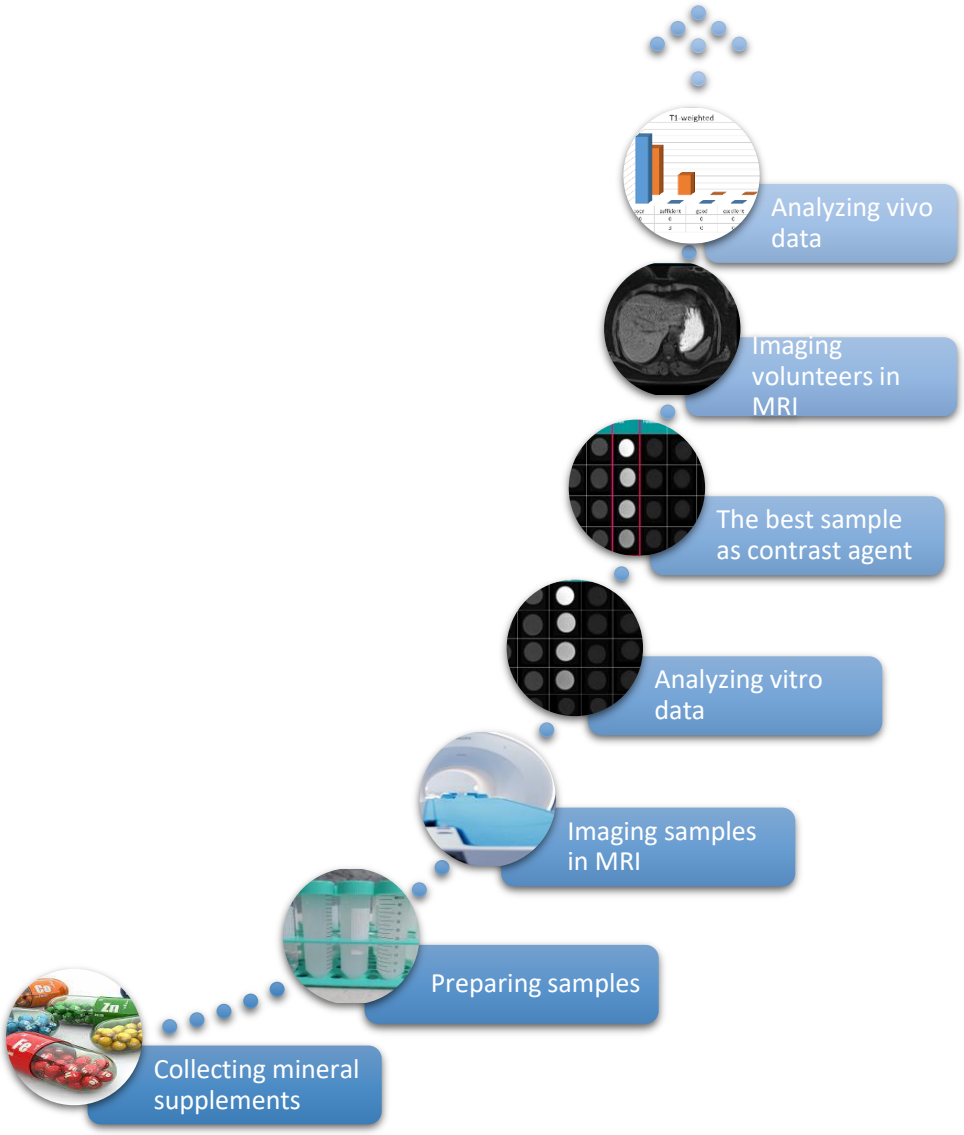

Figure 3. 4: Procedure of work

Chapter Three

The Results and Discussion

4.1 Introduction

In this chapter, we will present images and calculations derived from the study of the phantom, and the best sample will be chosen based on the results of the phantom study to be tested by volunteers. The magnetic resonance imaging system's image quality was assessed using quantitatively the signal intensity (*SI*), signal-to-noise ratio (*SNR*), relative signal-to-noise ratios (*RSN*), and contrast (*C*) of each volunteer's images. The qualitative assessment of *MR* images was performed using a questionnaire that was reviewed by a radiology specialist in *MRI*.

4.2 Concentration Measurement

The twenty-eight samples that have different mineral supplements with different concentrations have been tested by *TDS* meter to measure the concentration of mineral ions in water as shown in Table 4.1.

Table 4. 1: Concentration measurement of each sample. One cup=240 ml.

Number of samples	Amount of water (cup)	Calcium (ppm)	Zinc (ppm)	Iron (ppm)	Potassium (ppm)	Magnesium (ppm)	Sodium (ppm)	Manganese (ppm)
1	0.5	32	380	730	1350	172	1390	34
2	1	24	257	360	802	130	1102	15
2	1.5	19	178	316	700	119	780	7
4	2	15	100	240	510	106	581	3
5	(Distilled water)	0	0	0	0	0	0	0

4.3 The Results of the Phantom Study

4.3.1 *MR* Imaging of Phantoms

The twenty-eight samples that have different types of mineral supplements with different concentrations and seven samples of water (control) were examined by phantoms in *MRI* to obtain *T1*-weighted and *T2*-weighted scans at temperature=30℃ as shown in Figure 4.1 and Figure 4.2

Through the naked eye(qualitatively), it can be seen that the iron solutions significantly increased the signal intensity of water, and appeared bright white color on *T1*-weighted images (Figure 4.1), so it would be tested inside the human body in the next step. Manganese solutions also appeared with bright white color on *T1*-weighted but they are of less brightness than iron solutions. The rest of the solutions such as calcium, zinc, potassium, magnesium, and sodium did not show a significant visible color change in comparison with the water on the *T1*-weighted scan.

Figure 4.2 shows how the calcium solutions considerably enhanced the water's signal intensity and gave the image an illuminating white color on a *T2*-weighted scan, indicating that it would be invested in the test on volunteers in the following stage. On *T2*-weighted images, zinc likewise had a white appearance, albeit less so than calcium solutions.

Samples 1 and 2 of manganese in Figure 4.2 reduced the water signal completely and appeared black, so it can be considered a negative contrast agent and would not be tested inside the human body. Iron solutions also reduced the signal of water on *T2*- weighted and appeared with grey color but the signal reduction of iron solutions is less than that of manganese solutions. On a *T2*-weighted image, the other solutions (potassium, magnesium, and sodium) did not exhibit discernible changes in the color of the water.

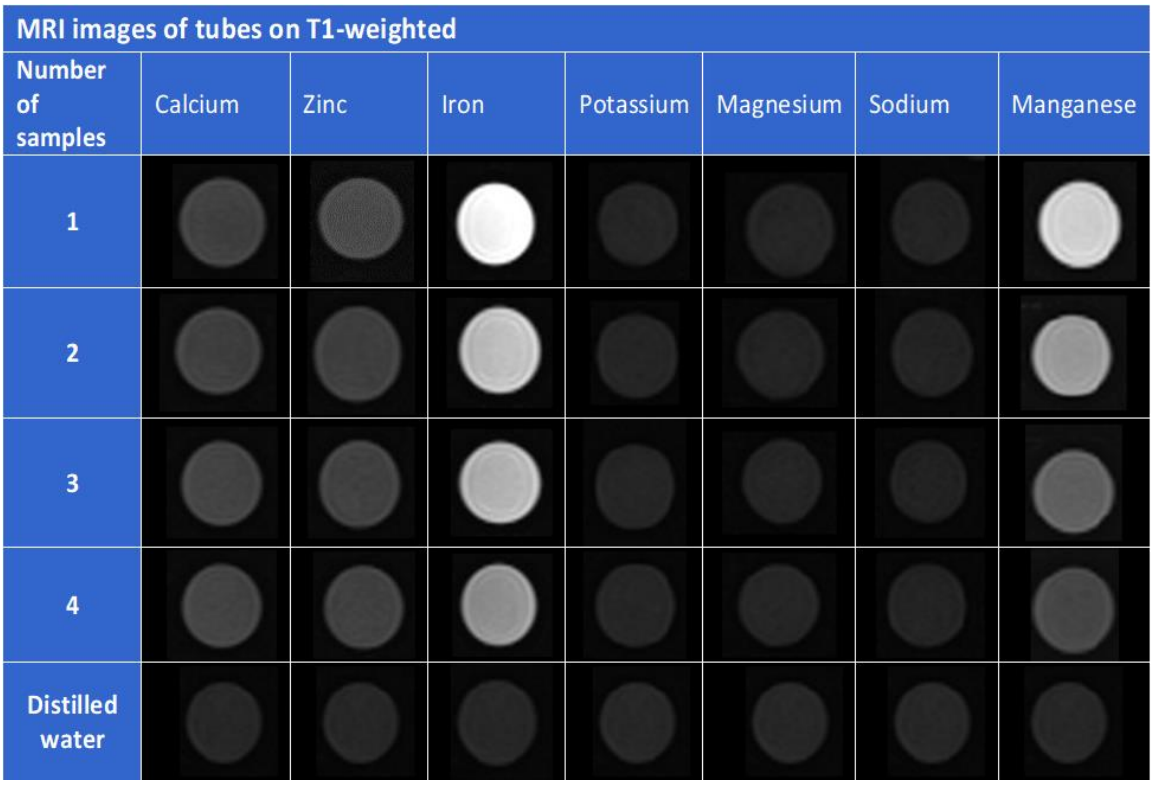

Figure 4.1: MRI images of phantoms on T1-weighted scan

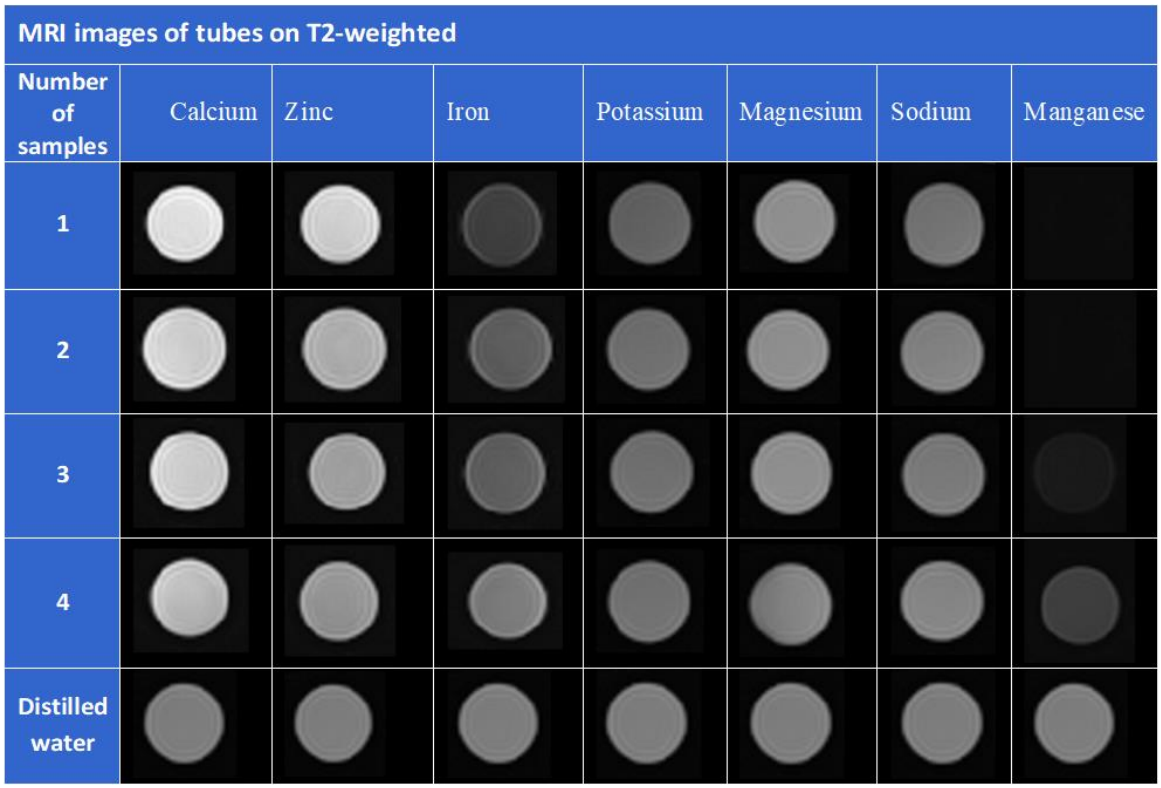

Figure 4.2: MRI images of phantoms on T2-weighted scan.

4.3.2 Characteristics of Phantoms *MR* Images

The fact that resolution in *MRI* is independent of input *RF* field wavelength is an intriguing feature. Actuality, the inherent resolution in *MRI* depends on how the signal and noise are sampled and filtered, and it is ultimately only constrained by the protons' diffusion through the tissue and the local nonuniformities in the magnetic field surrounding the proton. The metal supplement causes changes in the local magnetic field surrounding the proton of hydrogen [40]. Quantitative image evaluation through the determination of signal intensity was involved in the section on the optimal sample concentration for use as an oral contrast agent. Therefore, the signal intensity of each sample in Figures 4.1 and 4.2 is measured in Tables 4.2 and 4.3. Measurements were performed to calculate signal intensities by drawing the anatomical *ROI* 300 mm^2 area in *MR* images of phantoms.

Table 4. 2: The signal intensity of phantoms on T1-weighted scan

Number of samples	Signal intensity onT1-weighted						
	Calcium	Zinc	Iron	Potassium	Magnesium	Sodium	Manganese
1	197.50	196.42	851.74	93.18	93.27	89.31	590.44
2	195.54	192.52	637.52	92.4	92.55	89.12	450.9
3	194.98	190.33	586.45	91.53	91.25	88.80	264.28
4	192.63	189.23	470.71	90.70	91.03	88.76	159.95
Distilled water	88.41	88.41	88.41	88.41	88.41	88.41	88.41

We notice from Table 4.2 that the iron solutions give the highest signal intensity and they lie in the first order in this respect, while the manganese solutions are in the second order concerning the signal intensity height. In comparison to the other supplements, the water signal altered sufficiently little that the human eye was unable to recognize the difference.

Table 4.3: The signal intensity of phantoms on T2-weighted scan.

Number of Samples	Signal intensity on T2-weighted						
	Calcium	Zinc	Iron	Potassium	Magnesium	Sodium	Manganese
1	1093	982.50	267.27	330.85	495.43	394.72	0.15
2	988.86	804.63	401.42	380.43	495.16	418.74	0.69
3	974.19	735.73	410.70	382.09	492.41	448.01	35.44
4	871.97	652.25	418.05	387.33	491.47	453.10	124.31
Distilled water	454.78	454.78	454.78	454.78	454.78	454.78	454.78

In Table 4.3, the calcium solutions have the maximum signal intensity and they lie in the first order in this respect, whereas the zinc solutions lie in the second order concerning the signal intensity height. The water signal changes due to the other solutions are significantly less than the corresponding changes due to calcium and zinc solutions. Manganese solution as a reducing agent for the signal on *T2* images, completely dimmed the water signal in sample 1 and sample 2 of the manganese solutions, although the manganese solutions contain a small percentage of the manganese supplement.

The image's results were assessed using the *ROI* signal (area of 300 mm^2) and compared with background noise. On *T1*-weighted and *T2*-weighted images, the signal-to-noise ratio (*SNR*) for each sample was calculated according to equation (1.10), as shown in Tables 4.4 and 4.5. The images that have a low signal-to-noise ratio (*SNR*) or low signal intensity at a noise-level equivalent are neglected. Therefore, the image of sample 1 for the manganese solution is neglected on *T2*-weighted scan (Table 4.5).

Table 4. 4: The signal-to-noise ratio (SNR) of phantoms on T1- weighted scan.

Number of samples	SNR on T1-weighted						
	Calcium	Zinc	Iron	Potassium	Magnesium	Sodium	Manganese
1	194.79	193.71	849.03	90.47	90.56	86.60	587.73
2	192.83	189.81	634.81	89.69	89.84	86.41	448.19
3	192.27	187.62	583.74	88.82	88.54	86.09	261.57
4	189.92	186.52	468.00	87.99	88.32	86.05	157.24
Distilled water	85.70	85.70	85.70	85.70	85.70	85.70	85.70

Table 4.5: The signal-to-noise ratio (SNR) of phantoms on T2- weighted scan.

Number of samples	SNR on T2-weighted						
	Calcium	Zinc	Iron	Potassium	Magnesium	Sodium	Manganese
1	1092.46	981.96	266.73	330.31	494.89	394.18	-0.39
2	988.32	804.09	400.88	379.89	494.62	418.20	0.15
3	973.65	735.19	410.16	381.55	491.87	447.47	34.90
4	871.43	651.71	417.51	386.79	490.93	452.56	123.77
Distilled water	454.24	454.24	454.24	454.24	454.24	454.24	454.24

To assess the image of each sample qualitatively and quantitatively and to compare the signal of each sample with the water signal, equation (1.11) from the first chapter was used. The obtained relative signal-to-noise ratio (*RSN*) results are arranged in Table 4.6 and Table 4.7.

Table 4.6: The relative signal-to-noise ratio (RSN) of phantoms on T1-weighted scan.

Number of samples	RSN on T1-weighted						
	Calcium	Zinc	Iron	Potassium	Magnesium	Sodium	Manganese
1	2.27	2.26	9.91	1.06	1.06	1.01	6.86
2	2.25	2.21	7.41	1.05	1.05	1.01	5.23
3	2.24	2.19	6.81	1.04	1.03	1.00	3.05
4	2.22	2.18	5.46	1.03	1.03	1.00	1.83
Distilled water	1.00	1.00	1.00	1.00	1.00	1.00	1.00

In sample 1 of the iron solution, the presence of iron ions increased the water RSN by 9.91 times, as well as the rest of the iron samples increased the water RSN by 7.41, 6.81, and 5.46, the amount of increase is interesting, so it can be used as a positive contrast agent on *T1*-weighted images.

Table 4. 7: The relative signal-to-noise ratio (RSN) of phantoms on T2-weighted scan.

Number of samples	**RSN on T2-weighted**						
	Calcium	Zinc	Iron	Potassium	Magnesium	Sodium	Manganese
1	2.41	2.16	0.59	0.73	1.09	0.87	-0.0008
2	2.18	1.77	0.88	0.84	1.09	0.92	0.0003
3	2.14	1.62	0.90	0.84	1.08	0.99	0.0768
4	1.92	1.43	0.92	0.85	1.08	1.00	0.2724
Distilled water	1.00	1.00	1.00	1.00	1.00	1.00	1.00

In Table 4.7, the presence of calcium ions doubled the water signal. It can be utilized as a positive contrast agent on *T2*-weighted because of both the increase's quantity.

In the same table, it is seen that the presence of manganese ions reduced the water RSN significantly. For example, sample 2 of manganese reduced the RSN of water by 0.0003 times. The amount of reduction is significant, so it can be employed as a negative contrast agent on *T2*-weighted images.

The results of the phantoms study can be summarized as the following

- The calcium supplement causes a significant increase in the signal of the hydrogen (the water) on T2-weighted. Ca [$1s^2\ 2s^2\ 2p^6\ 3s^2\ 3p^6\ 4s^2$] is thought to be paramagnetic due to the excitation of one electron from the s orbital to the empty d orbital (the s and d orbitals are closer in energy, causing a transition to occur between both orbitals), rendering the s orbital unpaired in its excited state and attracted to the magnetic field (Pauli's paramagnetism) [82].
- The manganese supplement reduces the signal intensity of the hydrogen (the water) on *T2*-weighted. Manganese atom (Mn) has the following electron configuration: $1s^2\ 2s^2\ 2p^6\ 3s^2\ 3p^6\ 4s^2\ 3d^5$ [49]. In this instance, the manganese atom (*Mn*) has five unpaired electrons. This explains why there is a significant change in the signal strength despite the low manganese contents in the water.
- The iron supplement causes a significant increase in the signal of the hydrogen (the water) on *T1*-weighted. The electron configuration of the iron atom (*Fe)* is as follows: $1s^2\ 2s^2\ 2p^6\ 3s^2\ 3p^6\ 4s^2\ 3d^6$ [83]. The iron atom (Fe) in this case possesses four unpaired electrons. This explains why, despite few iron concentration in water, there is a considerable shift in the intensity of the signal.
- All concentrations of magnesium, potassium, and sodium supplements had no impact on the hydrogen signal in water. This is because when these materials dissolve in water, they form ions with saturated electronic shells unaffected by the magnetic field. For example, in sodium chloride ($NaCl$), ponding entails the transfer of an electron from each (Na) atom to (Cl) each the result two ions (Na^+ and Cl^- have close shells and are both diamagnetic [84].

The calcium, manganese, and iron supplements would be tested by volunteers.

4.4 The Results of the Volunteer Study

Thirty healthy participants had MRI scanning before and after the administration of a mineral supplement solution, after a 3-minute duration of administration, the participants were separated into three groups (each group consisted of ten volunteers). The first group took calcium supplements, the second group took manganese supplements, and the third group took iron supplements. The *MRI-GI* questionnaire was used for the qualitative analysis, which was evaluated by a radiologist, and the quantitative analysis was done by measuring the *SNR*, *RSN*, and contrast values.

4.4.1 The Calcium Supplement

a- *MR* Images

The study of calcium supplements includes five females and five males volunteers ranging in age from 25 to 35 years, with an average age of 29 years and a body mass index of 27.23 $Kg/m^{2,}$ ranging from 24.43 to 34.73 Kg/m^2. Following an eight-hour fast, the 10 healthy volunteers were subjected to two MRI exams; the imaging was performed on them before and after three minutes of drinking the best supplement solution. Images of participants were compared before and after the oral administration of the calcium supplement solution (2 calcium supplement tablets + 240 ml of water) to compare the MRI images of an empty stomach with MRI images of a stomach full of calcium solution as shown in Figure 4.3.

On the *T1*-weighted scan shown in Figure 4.3, the color of the stomach's interior did not change after drinking the calcium solution; however, on the *T2*-weighted scan, the stomach's interior changed color and appeared light grey.

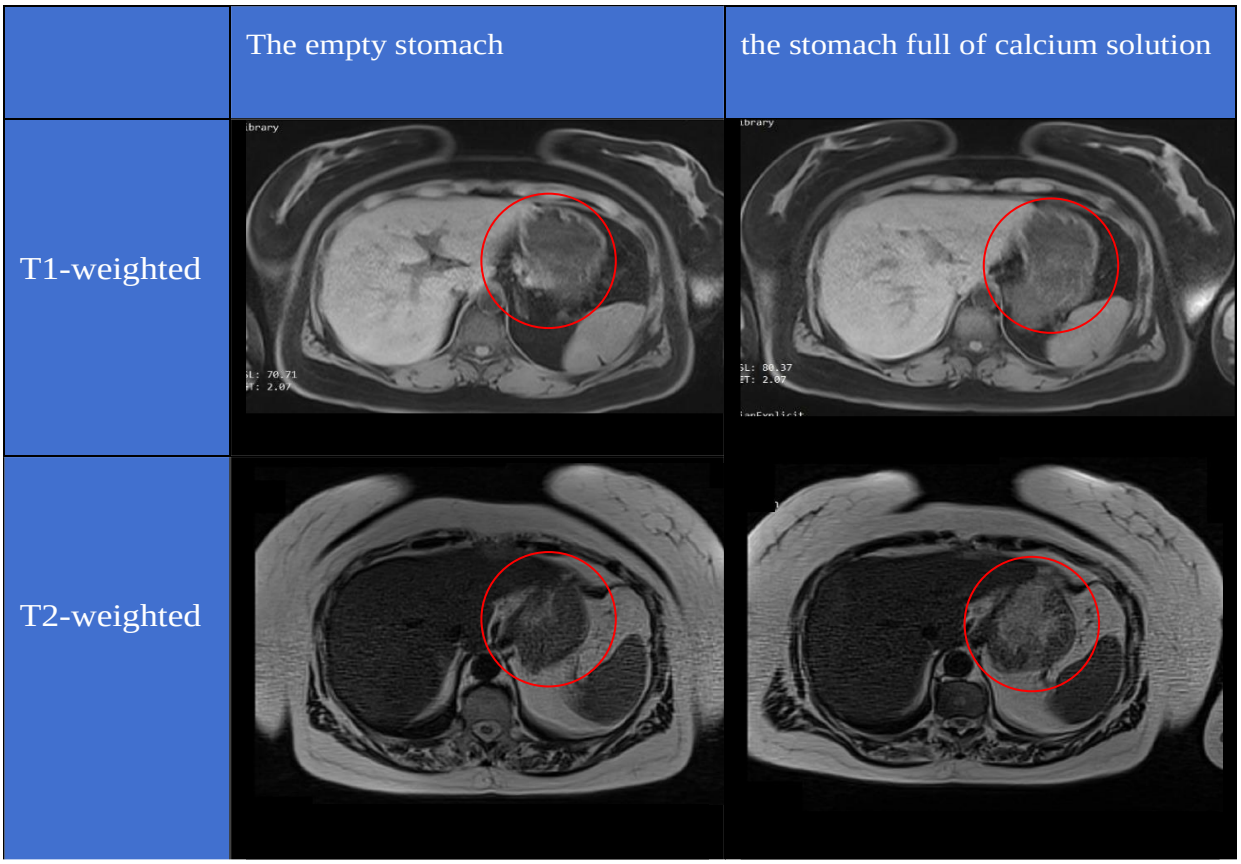

Figure 4.3: Transverse abdominal MRI for an empty stomach and a stomach full of calcium solution

b- Quantitative Analysis

To assess the image quality of the magnetic resonance equipment, the signal intensity (*SI*), signal-to-noise ratio (*SNR*), relative signal-to-noise ratios (*RSN*), and contrast (*C*) were evaluated using Equations (1.10) - (1.12) for each volunteer's before and after the oral administration. Signal intensities were calculated by drawing a 300 mm^2 area of interest (*ROI*) in the alimentary tract area for each participant.

The data of ten volunteers (two distinct sets were taken for each volunteer; before and after taking a calcium supplement solution) were gathered and calculated. The data were analyzed using *SPSS* (Statistical Package for Social Science) program.

The mean and standard deviation (*SD*) were used to estimate the quantitative data. Differences in qualities were explored using the t-test for quantitative data in a two-sets comparison. Both sides' P-values of 0.05 or less were regarded as statistically significant. Table 4.8 shows the statistical data of ten volunteers on the *T1*-weighted scan, whereas the volunteers' statistical data on *T2*-weighted images are shown in Table 4.9.

In Tables 4.8 and 4.9, the correlation values close to 1 indicate a linear positive correlation before and after taking calcium solution, and the P-value close to zero that means statistically highly significant. In the same tables, the presence of calcium had a positive effect on the hydrogen proton signal intensity and increased SNR, RSN, and contrast on T1-weighted and T2-weighted, but T2-weighted images have the highest contrast values.

Table 4. 8: The statistical data of Ten volunteers before and after taking a calcium supplement solution on T1-weighted.

	The empty stomach	The stomach full of calcium solution	Correlation	P-value
$SI_{mean} \pm SD$	96.18 ± 2.92	188.51 ± 4.17	0.762	$2.56*10^{-15}$
$SNR_{mean} \pm SD$	94.02 ± 2.93	186.38 ± 4.12	0.757	$2.46*10^{-15}$
$RSN_{mean} \pm SD$	1.17 ± 0.04	2.32± 0.05	0.757	$2.46*10^{-15}$
$C_{mean} \pm SD$	32.99 ± 4.33	125.32 ± 3.69	0.783	$2.56*10^{-15}$

Table 4. 9: The statistical data of Ten volunteers before and after taking a calcium supplement solution on T2-weighted

	The empty stomach	The stomach full of calcium solution	Correlation	P-value
$SI_{mean} \pm SD$	291.89 ± 4.45	828.67 ± 10.16	0.909	$7.76*10^{-19}$
$SNR_{mean} \pm SD$	290.12 ± 4.45	826.95 ± 10.22	0.907	$8.48*10^{-19}$
$RSN_{mean} \pm SD$	0.68 ± 0.01	1.94 ± 0.02	0.907	$8.48*10^{-19}$
$C_{mean} \pm SD$	145.96 ± 1.58	682.72 ± 7.80	0.875	$8.50*10^{-19}$

Qualitative Analysis

The qualitative assessment of MR images was performed using a questionnaire that was reviewed by a radiology specialist, and the data from the image assessment findings were analyzed. Questionnaires on the anatomy of gastrointestinal contrast were completed using the Likert scale: -

1= poor, 2= sufficient, 3= good, 4= excellent.

The qualitative evaluations of *MR* images on *T1*-weighted and *T2*-weighted are shown in Figures 4.4 and 4.5.

Figure (4.4) displays the radiologist assessment of gastrointestinal tract images on *T1*-weighted. In that graph, the entire gastrointestinal tract had a value of poor without calcium supplement treatment, and the majority also had a value

of bad following calcium supplementation. This indicates the ineffectiveness of calcium supplementation as a contrast agent on *T1*-weighted images.

The graph in Figure (4.5) depicts the evaluation of the gastric tract images. In this graph, the majority of the gastric tract had a value of poor without calcium supplement administration; however, the majority obtained a value of good after calcium supplementation.

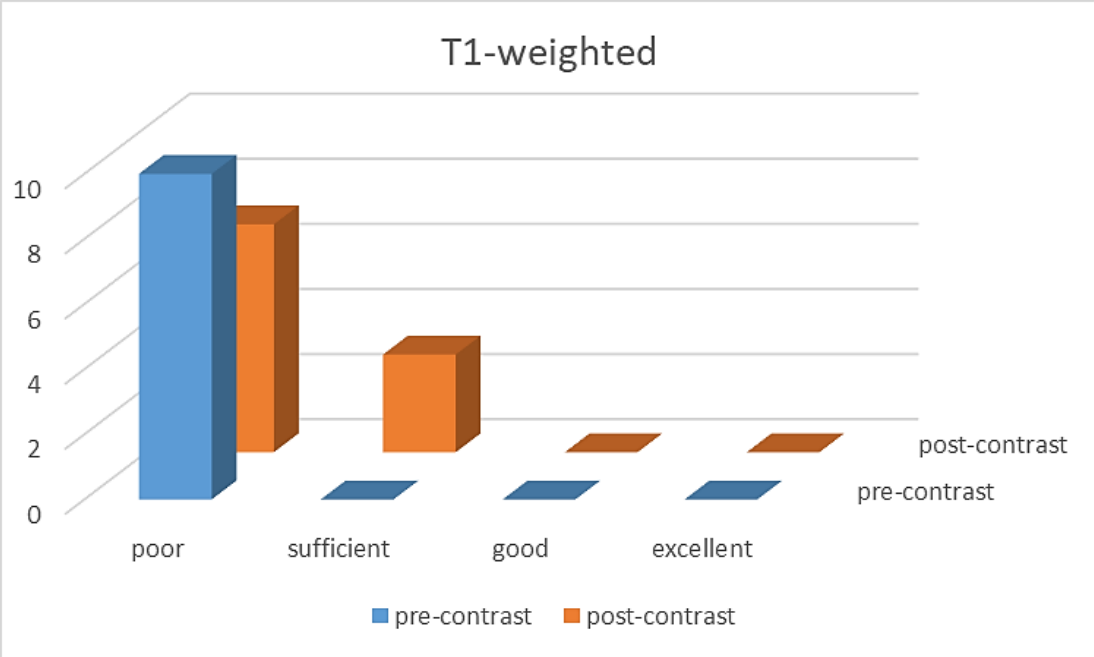

Figure 4.4: The comparison of MR images before and after calcium supplement solution administration on T1-weighted scan.

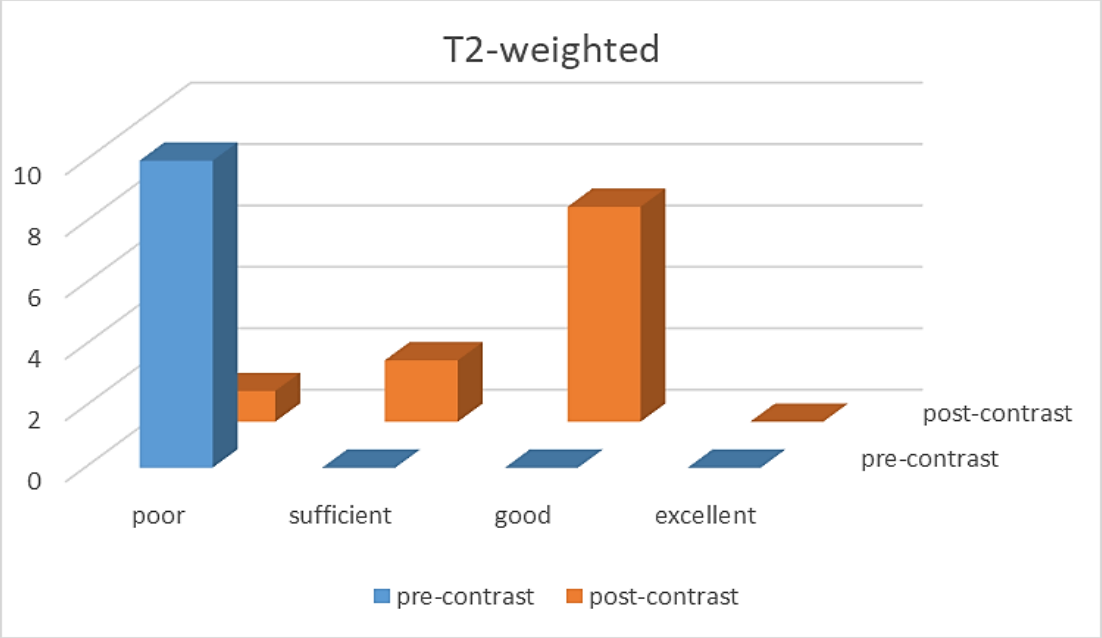

Figure 4.5: The comparison of MR images before and after calcium supplement solution administration on T2-weighted scan.

The calcium supplement significantly increases the hydrogen (water) signal on T2-weighted imaging. *Ca* [$1s^2$ $2s^2$ $2p^6$ $3s^2$ $3p^6$ $4s^2$] is believed to be paramagnetic because of the excitation of one electron from the s orbital to the emptied d orbital (the s and d orbitals are closer in energy, causing a transition to occur between both orbitals), leaving the s orbital unpaired in its excited state and attracted to the magnetic field (Pauli's paramagnetism) [48].

The quantitative and qualitative evaluation of the *MR* images demonstrate the utility of calcium supplementation as a positive contrast agent on T2-weighted.

4.4.2 The Manganese Supplement

a- *MR* Images

With an average age of 33.6 years and a body mass index of 27.42 kg/m^2, ranging from (23.63 - 27.18) kg/m^2, the six females and four males participants in the trial of manganese supplements range in age from 23 to 47 years. The ten healthy participants underwent two *MRI* tests after an eight-hour fast; the imaging was done on them before and after they drank the manganese supplement solution lasting 3 minutes.

Figure 4.6 shows the comparison of *MRI* scans for an empty stomach and MRI scans for a stomach full of manganese solution taken before and after the oral administration of the manganese supplement solution (one manganese supplement tablet + 240 ml of water).

The stomach's interior on the *T1*-weighted scan seen in Figure 4.6 changed color and appeared bright white. The stomach's interior changed color and appeared black on the *T2*-weighted scan after drinking the manganese solution.

	The empty stomach	the stomach full of manganese solution
T1-weighted	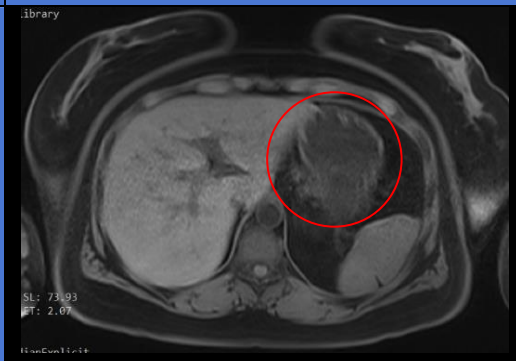	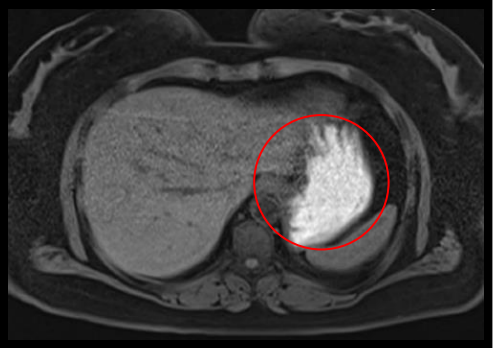
T2-weighted	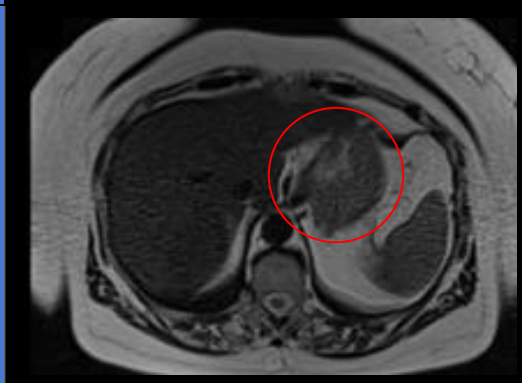	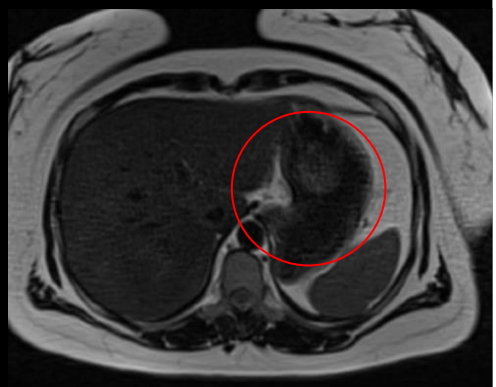

Figure 4. 6: Transverse abdominal MRI for an empty stomach and a stomach full of manganese solution

b- Quantitative Analysis

The image quality of the magnetic resonance equipment was assessed using the signal intensity (*SI*), signal-to-noise ratio (*SNR*), relative signal-to-noise ratios (*RSN*), and contrast (*C*) of each volunteer's subjected to two tests. Drawing a 300 mm^2 region of interest (*ROI*) in the area of the gastrointestinal tract for each participant allowed us to compute the signal intensities.

Data were collected and calculations were made for two separate sets of ten participants (before and after consuming a manganese supplement solution). The

SPSS application was used to analyze the data. The quantitative values were estimated using the mean and standard deviation (*SD*). The t-test for quantitative data was used in a two-set comparison to examine quality differences. P-values of 0.05 or less for both sides were considered statistically significant. Ten subjects' statistical data on *T1*-weighted images are displayed in Table 4.10, while volunteers' statistical data on *T2*-weighted images are displayed in Table 4.11.

In Tables 4.10 and 4.11, correlation values around 1 demonstrate a linear positive correlation before and after drinking manganese solution, while P-values near 0 imply highly statistical significance.

Reduced *T2* relaxation time, which results in lower signal intensity from the manganese supplement fluid than stomach tissues on *T2*-weighted imaging, is what gives the manganese supplement solution its negative contrast impact.

Table 4.10: The statistical data of ten volunteers before and after taking a manganese supplement solution on T1-weighted scan.

	The empty stomach	the stomach full of manganese solution	correlation	P-value
$SI_{mean} \pm SD$	96.18 ± 2.80	426.81 ± 2.51	0.99	$2.57*10^{-25}$
$SNR_{mean} \pm SD$	93.18 ± 2.47	424.42 ± 2.15	0.95	$3.00*10^{-25}$
$RSN_{mean} \pm SD$	1.16± 0.03	5.31 ± 0.03	0.95	$3.00*10^{-25}$
$C_{mean} \pm SD$	33.29±3.93	363.62 ± 4.17	0.93	$2.12*10^{-22}$

Table 4.11: *The statistical data of ten volunteers before and after taking a manganese supplement solution on T2-weighted scan.*

	The empty stomach	the stomach full of manganese solution	correlation	P-value
$SI_{mean} \pm SD$	291.19 ± 4.94	56.77 ± 3.41	0.72	$4.67*10^{-18}$
$SNR_{mean} \pm SD$	287.28 ± 4.83	51.10 ± 3.57	0.80	$1.05*10^{-18}$
$RSN_{mean} \pm SD$	0.68 ± 0.01	0.12 ± 0.01	0.80	$8.21*10^{-21}$
$C_{mean} \pm SD$	145.42 ± 3.47	-78.27 ±3.65	0.95	$3.36*10^{-22}$

c- Qualitative Analysis

The radiology specialist assessed the data from the image evaluation findings, and the qualitative assessment of *MR* images was completed using a questionnaire. The Likert scale was used to complete questionnaires on the contrast between the gastrointestinal system and the manganese solution. The figures below illustrate the qualitative evaluation of *T1*-weighted and *T2*-weighted *MR* images.

Figure 4.7 represents the radiology specialist's evaluation of T1-weighted gastrointestinal tract images. In this graph, the wall of the gastric tract had a bad value without manganese supplementation, while the majority had an excellent value after manganese treatment. This demonstrates the utility of manganese administration as a positive contrast agent on T1-weighted.

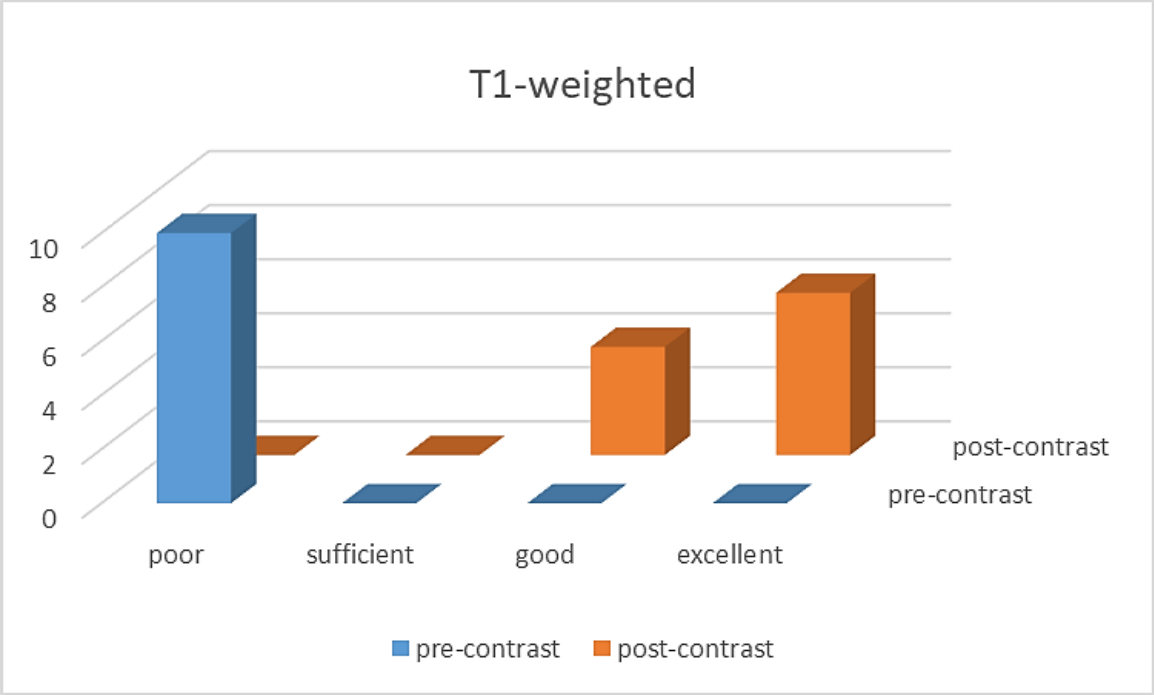

Figure 4.7: The comparison of MR images before and after manganese supplement solution administration on T1-weighted scan.

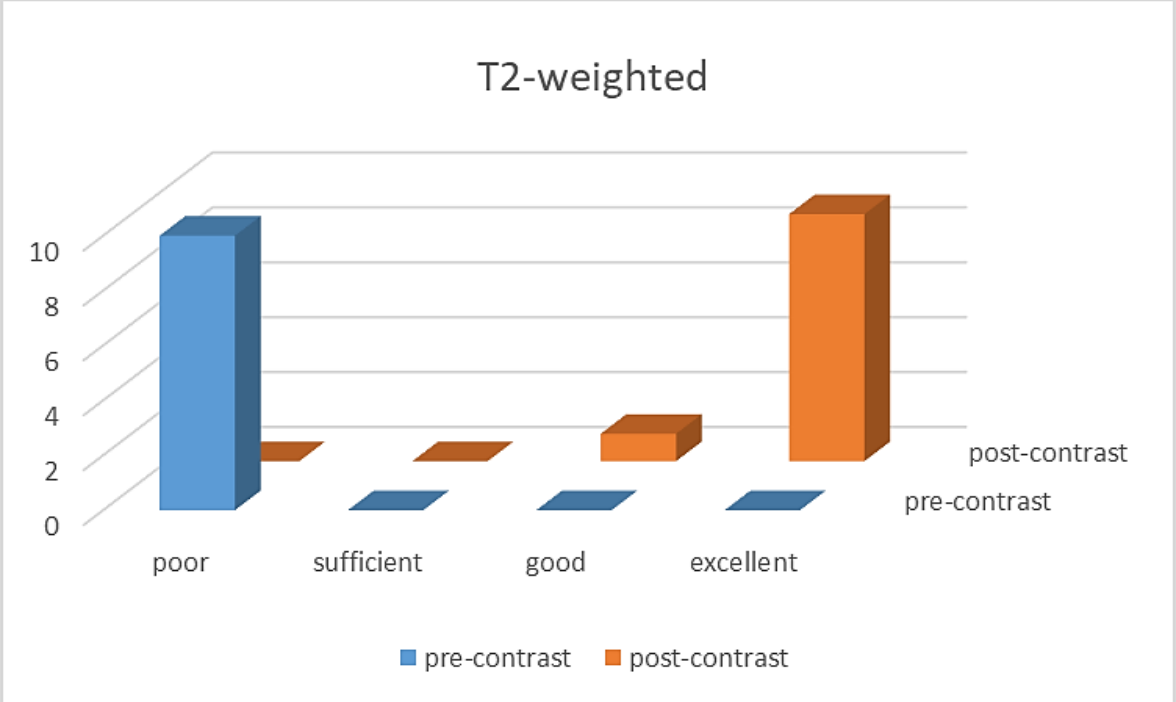

Figure 4.8: The comparison of MR images before and after manganese supplement solution administration on T2-weighted scan.

The bulk of the graph in Figure 4.8 showed an excellent value following manganese supplementation. This indicates the value of the manganese supplement as a negative contrast agent on T2-weighted.

The quantitative and qualitative analysis of the *MR* images supports the efficacy of manganese supplementation as a positive contrast agent on *T1*-weighted images and negative contrast agent on *T2*-weighted images. This result is consistent with the results obtained by previous studies such as the work performed by Utami *et al* [53], carried out the first experimental investigation using jasmine (Contains a high concentration of manganese) as oral contrast agent. This study demonstrated that jasmine tea may be utilized as a substitute safe natural negative oral contrast agent on *T2*-weighted, and Vesna *et al* [54], employed pineapple juice (contains a high concentration of manganese) instead of commercially available negative contrast agents on *T2*-weighted scan via *MRI*. The manganese supplement increases the hydrogen (water) signal intensity on T1-weighted images and decreases it on *T2*-weighted images. The electron configuration of manganese atom (*Mn*) is as the following: $1s^2$, $2s^2$, $2p^6$, $3s^2$, $3p^6$, $4s^2$, $3d^5$ [49]. The manganese atom (*Mn*) in this case possesses five unpaired electrons. This explains why there is a significant difference in signal intensity despite the low manganese concentration in the water. This indicates the manganese administration's importance as a positive contrast agent on a *T1*-weighted scan and a negative contrast agent on a *T2*-weighted scan.

4.4.3 The Iron Supplement

a- *MR* Images

The five female and five male participants in the iron supplement experiment vary in age from 24 to 58 years, with an average age of 37.7 years and a body mass index of 27.95 kg/m^2 ranging from (22.96 - 31.93) kg/m^2. After an eight-hour fast,

the 10 healthy individuals got two *MRI* exams; the imaging was performed on them before and after they drank the iron supplement solution.

Figure 4.9 depicts a comparison of *MRI* scans performed before and after oral administration of the iron supplement solution (one iron supplement tablet + 240 ml of water) for an empty stomach and *MRI* scans taken after oral administration of the iron supplement solution for a stomach full of iron solution.

The color of the stomach's contents changed to bright white on the *T1*-weighted scan as depicted in Figure 4.9. The stomach's contents changed color and appeared grey on the *T2*-weighted scan after consuming the iron solution.

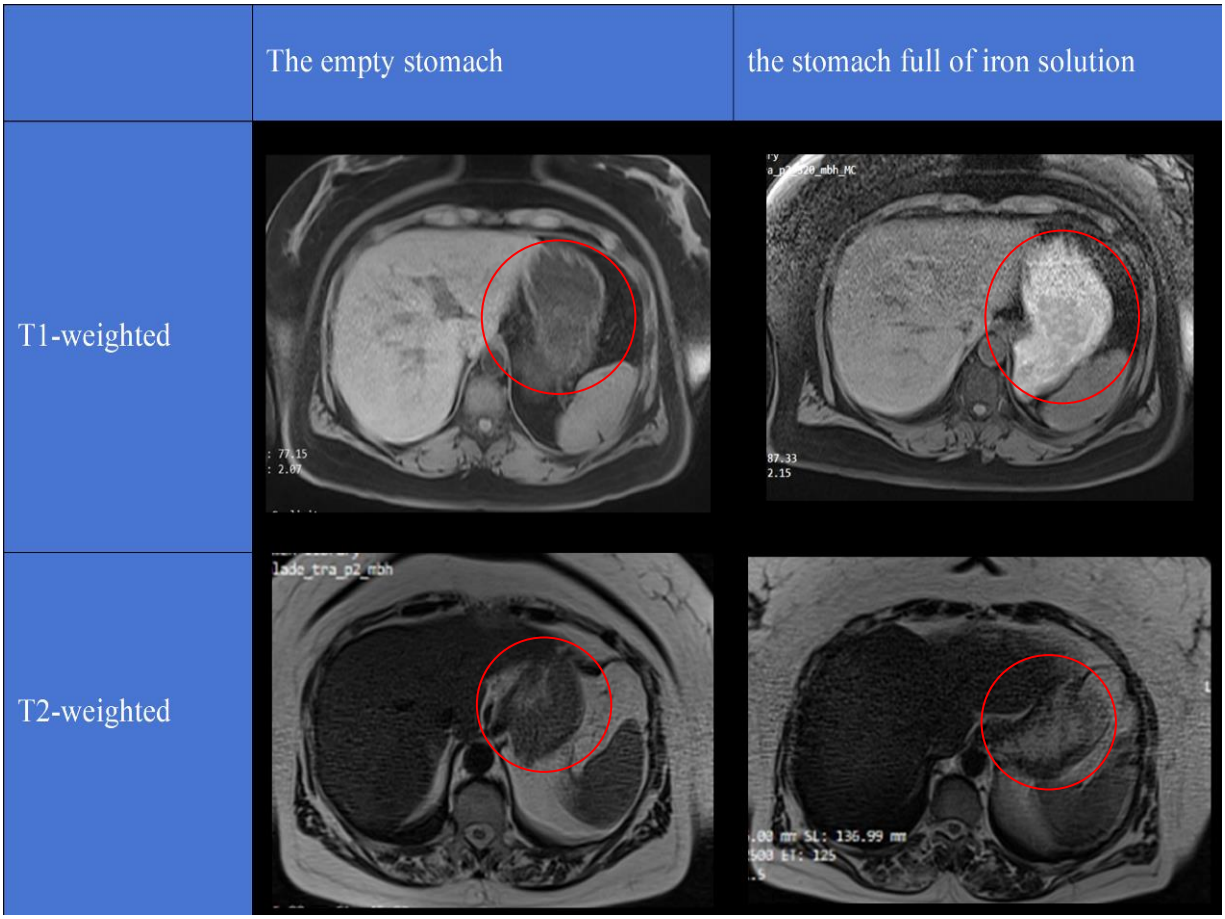

Figure 4.9: Transverse abdominal MRI for an empty stomach and a stomach full of iron solution

b- Quantitative Analysis

We calculated signal intensities by drawing a 300 mm^2 region of interest (*ROI*) in the area of the stomach and intestines for each participant. For each volunteer, the signal-to-noise ratio (*SNR*), relative signal-to-noise ratios (*RSN*), and contrast (*C*) were measured.

Data and computations were obtained for two distinct groups of ten volunteers (before and after taking an iron supplement solution). The data were analyzed using the SPSS program. The mean and standard deviation (*SD*) were used to estimate the quantitative values. In a two-set comparison, the t-test for quantitative data was utilized to investigate quality differences. P-values ≤ 0.05 were deemed statistically significant on both sides.

Table 4.12 displays statistical data from ten individuals on *T1*-weighted images, whereas Table 4.13 displays statistical data from volunteers on *T2*-weighted images.

Table 4. 12: The statistical data of ten volunteers before and after taking an iron supplement solution on T1-weighted scan.

	The empty stomach	**the stomach full of iron solution**	**correlation**	**P-value**
$SI_{mean} \pm SD$	95.89 ± 2.58	498.41 ± 1.97	0.825	$1.86*10^{-23}$
$SNR_{mean} \pm SD$	92.89 ± 2.27	496.02± 1.74	0.817	$6.94*10^{-24}$
$RSN_{mean} \pm SD$	1.16 ± 0.03	6.18± 0.02	0.817	$6.94*10^{-24}$
$C_{mean} \pm SD$	33.00± 3.96	435.22 ± 3.80	0.859	$3.88*10^{-22}$

Table 4. 13: The statistical data of ten volunteers before and after taking an iron supplement solution on T2-weighted scan.

	The empty stomach	the stomach full of iron solution	correlation	P-value
$SI_{mean} \pm SD$	291.18 ± 4.93	395.36 ± 2.94	0.924	$4.03*10^{-16}$
$SNR_{mean} \pm SD$	287.28 ± 4.82	389.70 ± 3.54	0.877	$3.62*10^{-16}$
$RSN_{mean} \pm SD$	0.68 ± 0.01	0.92 ± 0.008	0.877	$3.62*10^{-16}$
$C_{mean} \pm SD$	145.42 ± 3.47	260.33 ± 3.45	0. 799	$1.13*10^{-16}$

The correlation values around 1 in Tables 4.12 and 4.13 show a linear positive correlation before and after ingesting iron solution, and the P-value near 0 indicates statistically highly significant results.

c- Qualitative Analysis

The radiology professional evaluated the data from the image evaluation findings, and the qualitative assessment of *MR* images was conducted using a questionnaire. The Likert scale was utilized to answer questionnaires on the contrast between the stomach and intestines and the manganese solution. Figures 4.10 and 4.11 show the qualitative evaluation of *T1*-weighted and *T2*-weighted *MR* images.

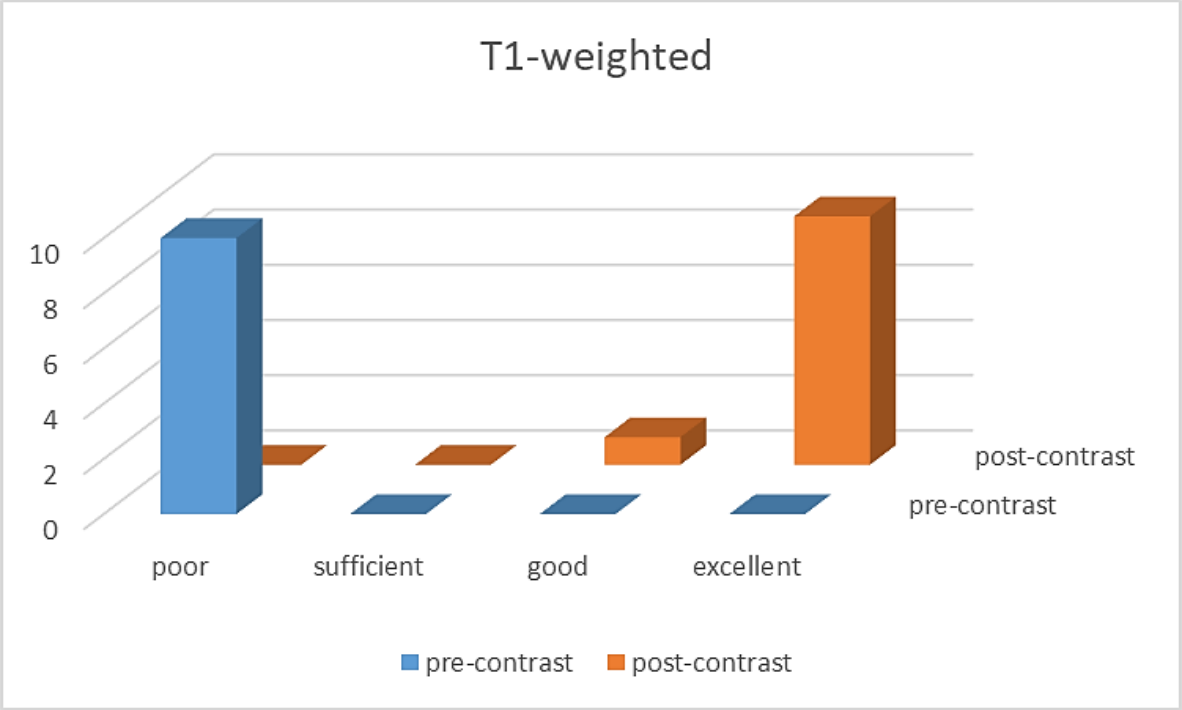

Figure 4.10: The comparison of MR images before and after iron supplement solution administration on T1-weighted scan.

T1-weighted images of the gastrointestinal system are evaluated by the radiology specialist in Figure 4.10. Without iron addition, the gastrointestinal tract wall had a poor value in that graph, but the majority had an excellent score following iron treatments. This indicates the value of iron treatment as a positive contrast agent.

The examination of the stomach images is shown in Figure 4.11. After iron supplementation, the majority of those on that graph attained a sufficient evaluation. This demonstrates that iron supplementation may be used as a negative contrast agent. However, manganese is more effective as a negative contrast agent on *T2*-weighted scan.

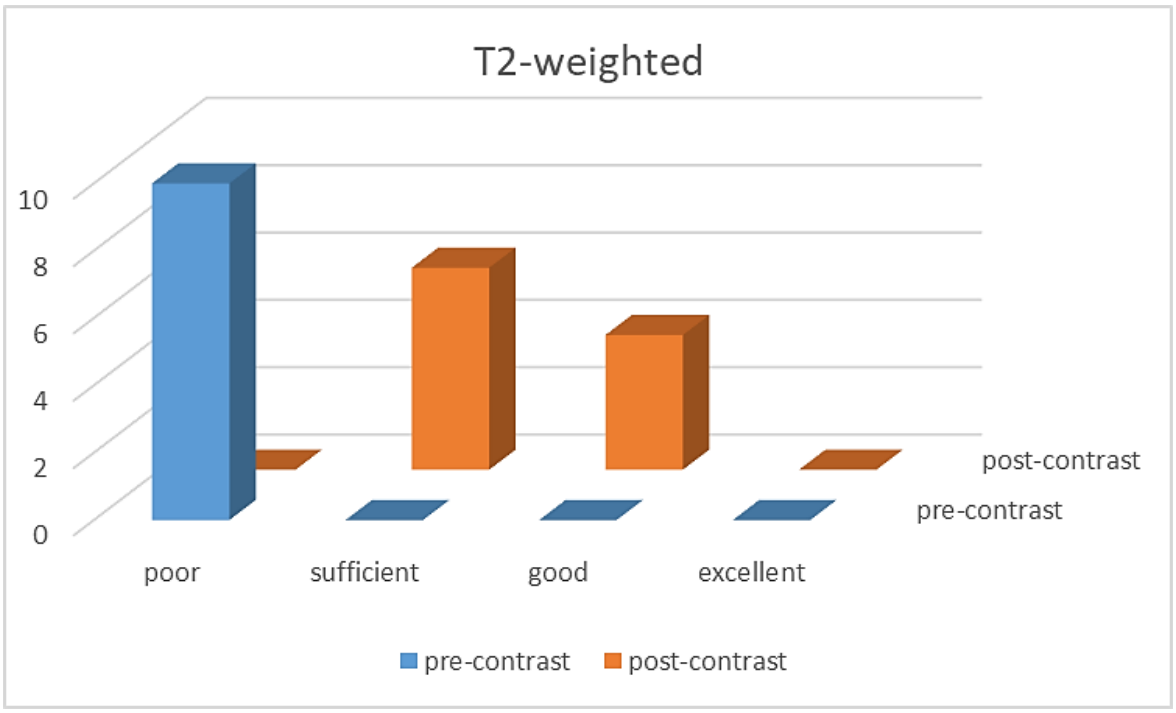

Figure 4.11: The comparison of MR images before and after iron supplement solution administration on T1-weighted scan.

The effectiveness of iron supplementation as a positive contrast agent on *T1*-weighted images and a negative contrast agent on *T2*-weighted images is supported by the quantitative and qualitative analysis of the *MR* images. This result is in agreement with studies performed by other researchers like Isnoviasih *et al* [50] who used superparamagnetic iron supplement solutions as a replacement for negative contrast media. This study compared the variations in stomach *SNR* values on *T2*-weighted before and after administering an iron supplement solution as a substitute for negative oral contrast media.

The iron supplement significantly enhances the hydrogen (water) signal on *T1*-weighted and reduces T2-weighted imaging. Iron atom (*Fe*) electron arrangement is as the following: $1s^2$, $2s^2$, $2p^6$, $3s^2$, $3p^6$, $4s^2$, $3d^6$ [49]. In this situation, the iron ion has four unpaired electrons. This explains why, despite the low

concentration of iron in the water, there is a significant change in signal intensity. As a result, it can be shown that iron supplements can act as a positive media on *T1*-weighted and a negative media on *T2*-weighted. On *T2*-weighted images, manganese performs more efficiently as a negative media.

Chapter Five

The Conclusions

5.1 Conclusions

The previously conducted results and analysis can be summarized by the conclusions below.

1. A positive contrast agent on T2-weighted images might be the calcium supplement. Zinc acts less efficiently as a positive contrast agent on T2-weighted images.
2. The significance of the manganese supplementation as a positive contrast agent on a T1-weighted scan and a negative contrast agent on a T2-weighted images.
3. The iron supplement has a substantial beneficial effect on T1-weighted images and a negative effect on T2-weighted images. Manganese operates more efficiently as a negative medium on T2-weighted images.
4. Magnesium, potassium, and sodium supplements had no significant effect on T1-weighted and T2-weighted images.

5.2 Recommendations

There are some important recommendations for anyone interested in the field of magnetic resonance imaging:

1. Manganese and iron supplements are excellent positive contrast agents on *T1*-weighted. Manganese supplement is an effective negative contrast agent and calcium supplement is a beneficial positive contrast agent that may be used for gastrointestinal tests on *T2*-weighted images.
2. If mineral supplements are used as an oral contrast agent, the patient must have a blood test done beforehand to find out if he has an excess of a certain mineral.

5.3 Future works

Through the scientific process of this research, some future works can be proposed:

1. Some mineral supplements (such as calcium, manganese, and iron) can be given intravenously so that they may be studied as an intravenous contrast agent.
2. Study another mineral supplement such as copper supplement as a contrast agent in MRI
3. Preparation of mineral supplements as nanomaterials and study of their properties.
4. Study of higher doses of mineral supplements instead of intake daily dose.

References

1. Zarrini, M., Seilanian Toosi, F., Davachi, B., Nekooei, S. Natural oral contrast agents for gastrointestinal magnetic resonance imaging. Reviews in Clinical Medicine, 2015; 2(4): 200-204. DOI: 10.17463/RCM.2015.04.009
2. Maqbool M. An Introduction to Medical Physics. 2017. URL http://www. springer. com/series/3740.
3. Mackalski BA, Bernstein CN. New diagnostic imaging tools for inflammatory bowel disease. Gut. 2006 May 1;55(5):733-41.
4. Dohan A, Faraoun SA, Barral M, Guerrache Y, Boudiaf M, Dray X, Hoeffel C, Allez M, Farges O, Beaugerie L, Aparicio T. Extra-intestinal malignancies in inflammatory bowel diseases: An update with emphasis on MDCT and MR imaging features. Diagnostic and interventional imaging. 2015 Sep 1;96(9):871-83.DOI: 10.1016/j.diii.2015.02.009
5. Koplay M, Guneyli S, Cebeci H, Korkmaz H, Emiroglu HH, Sekmenli T, Paksoy Y. Magnetic resonance enterography with oral mannitol solution: Diagnostic efficacy and image quality in Crohn disease. Diagnostic and interventional imaging, 2017 Dec 1;98(12):893-9. DOI: 10.1016/j.diii.2017.06.011.
6. Merbach AS, Helm L, Toth E. The chemistry of contrast agents in medical magnetic resonance imaging. John Wiley & Sons; 2013 Feb 19. DOI:10.1002/9781118503652.
7. Villa A, Hess B, Saint-Martin H. Dynamics and structure of Ln (III)− aqua ions: a comparative molecular dynamics study using ab initio based flexible and polarizable model potentials. The Journal of Physical Chemistry B. 2009 May 21;113(20):7270-81. DOI: 10.1021/jp8097445.

8. Hammes GG. Physical chemistry for the biological sciences. John Wiley & Sons; 2007 Apr 10.
9. Dale BM, Brown MA, Semelka RC. MRI: basic principles and applications. John Wiley & Sons; 2015 Aug 6.
10. Burtea C, Laurent S, Vander Elst L, Muller RN. Contrast agents: magnetic resonance. Molecular imaging I. 2008:135-65. DOI:10.1007/978-3-540-72718-7_7.
11. Bushberg JT, Boone JM. The essential physics of medical imaging. Lippincott Williams & Wilkins; 2011 Dec 20.
12. Plewes DB, Kucharczyk W. Physics of MRI: a primer. Journal of magnetic resonance imaging. 2012 May;35(5):1038-54.DOI: 10.1002/jmri.23642
13. Weishaupt D, Köchli VD, Marincek B, Froehlich JM, Nanz D, Pruessmann KP. How does MRI work?: an introduction to the physics and function of magnetic resonance imaging. Berlin: Springer; 2006 Jul 1.
14. Davidovits P. Physics in biology and medicine. Academic Press; 2018 Nov 28.
15. Barnes FS, Greenebaum B, editors. Biological and medical aspects of electromagnetic fields. CRC press; 2018 Oct 3.
16. Brown RW, Cheng YC, Haacke EM, Thompson MR, Venkatesan R. Magnetic resonance imaging: physical principles and sequence design. John Wiley & Sons; 2014 Jun 23.
17. Landini L, Positano V, Santarelli M, editors. Advanced image processing in magnetic resonance imaging. CRC press; 2018 Oct 3.
18. Kuperman V. Magnetic resonance imaging: physical principles and applications. Elsevier; 2000 Mar 15.
19. Hobbie RK, Roth BJ. Intermediate physics for medicine and biology. Springer Cham; 2015. DOI:10.1007/978-3-319-12682-1

20. Smith NB, Webb A. Introduction to medical imaging: physics, engineering and clinical applications. Cambridge university press; 2010 Nov 18.
21. Rule GS, Hitchens TK. NMR spectroscopy. Springer Netherlands; 2006. DOI: 10.1007/1-4020-3500-4_1.
22. Hendee WR, Morgan CJ. Magnetic resonance imaging Part I—Physical principles. Western Journal of Medicine. 1984 Oct;141(4):491.
23. Demir A. NMR-the basic principles and its use in studies of water/ethanol/mixture;2012.
24. Sprawls P. Magnetic resonance imaging: principles, methods, and techniques. Madison: Medical Physics Publishing; 2000 Jul 1.
25. Vassiliou VS, Cameron D, Prasad SK, Gatehouse PD. Magnetic resonance imaging: Physics basics for the cardiologist. JRSM cardiovascular disease. 2018 May; 7:2048004018772237. DOI: 10.1177/2048004018772237.
26. Brown MA, Semelka RC. MRI: basic principles and applications. John Wiley & Sons; 2011 Jan 14.
27. Hargreaves B. Rapid gradient-echo imaging. Journal of Magnetic Resonance Imaging. 2012 Dec;36(6):1300-13.
28. Chavhan GB, Babyn PS, Jankharia BG, Cheng HL, Shroff MM. Steady-state MR imaging sequences: physics, classification, and clinical applications. Radiographics. 2008 Jul;28(4):1147-60. DOI: 10.1148/rg.284075031
29. Bernstein MA, King KF, Zhou XJ. Handbook of MRI pulse sequences. Elsevier; 2004 Sep 21.
30. Mills AF, Sakai O, Anderson SW, Jara H. Principles of quantitative MR imaging with illustrated review of applicable modular pulse diagrams. RadioGraphics. 2017 Nov;37(7): 2083-105.DOI: 10.1148/rg.2017160099.

31.Hanrahan CJ, Shah LM. MRI of spinal bone marrow: part 2, T1-weighted imaging-based differential diagnosis. American Journal of Roentgenology. 2011 Dec;197(6):1309-21. DOI:10.2 214 /A JR.11.7420.

32.Westbrook C. Handbook of MRI technique. John Wiley & Sons; 2008.

33.Lv J, Roy S, Xie M, Yang X, Guo B. Contrast Agents of Magnetic Resonance Imaging and Future Perspective. Nanomaterials. 2023 Jul 4;13(13):2003. DOI: 10.1021/acsanm.2c03297.

34. Wahsner J, Gale EM, Rodríguez-Rodríguez A, Caravan P. Chemistry of MRI contrast agents: current challenges and new frontiers. Chemical reviews. 2018 Oct 16;119(2):957-1057. DOI: 10.1021/acs.chemrev.8b00363.

35.Li KC, Tart RP, Fitzsimmons JR, Storm BL, Mao J, Rolfes RJ. Barium sulfate suspension as a negative oral MRI contrast agent: in vitro and human optimization studies. Magnetic resonance imaging. 1991 Jan 1;9(2): 141-50.DOI: 10.1016/0730-725X(91)90002-4.

36. Kochanek PM, Tasker RC, Carney N, Totten AM, Adelson PD, Selden NR, Davis-O'Reilly C, Hart EL, Bell MJ, Bratton SL, Grant GA. Guidelines for the management of pediatric severe traumatic brain injury: update of the brain trauma foundation guidelines. Pediatric Critical Care Medicine. 2019 Mar 1;20(3S): S1-82. DOI: 10.1097/PCC.0000000000001735.

37.Qin R, Li S, Qiu Y, Feng Y, Liu Y, Ding D, Xu L, Ma X, Sun W, Chen H. Carbonized paramagnetic complexes of Mn (II) as contrast agents for precise magnetic resonance imaging of sub-millimeter-sized orthotopic tumors. Nature Communications. 2022 Apr 11;13(1):1938. DOI: 10.1038/s41467-022-29586-w.

38.Cullity BD, Graham CD. Introduction to magnetic materials. John Wiley & Sons; 2011 Oct 7.

39. Arthurs OJ, Graves MJ, Edwards AD, Joubert I, Set PA, Lomas DJ. Interactive neonatal gastrointestinal magnetic resonance imaging using fruit juice as an oral contrast media. BMC medical imaging. 2014 Dec;14: 1-8. DOI: 10.1186/1471-2342-14-33.

40. Avila PJ. Biomedical applications of inorganic nanoparticles: Magnetic Resonance Imaging and Hyperthermia [PhD thesis]. University of Milano-Bicocca: Bicocca Open Archive; 2015.

41. Milotta G, Green I, Roiser JP, Callaghan MF. In vivo multi-parameter mapping of the habenula using MRI. Scientific Reports. 2023 Mar 7;13(1):3754.DOI: 10.1038/s41598-023-28446-x.

42. Liu J, Pan Y, Li M, Chen Z, Tang L, Lu C, Wang J. Applications of deep learning to MRI images: A survey. Big Data Mining and Analytics. 2018 Jan 25;1(1):1-8. DOI: 10.26599/BDMA.2018.9020001

43. Riordan RD, Khonsari M, Jeffries J, Maskell GF, Cook PG. Pineapple juice as a negative oral contrast agent in magnetic resonance cholangiopancreatography: a preliminary evaluation. The British journal of radiology. 2004 Dec;77(924):991-9. DOI: 10.1259/bjr/36674326.

44. Espinosa MG, Sosa M, De León-Rodríguez LM, Córdova T, Bernal-Alvarado J, Avila-Rodríguez M, Reyes-Aguilera JA, Ortíz JJ, Barrios FA. Blackberry (Rubus spp.): a pH-dependent oral contrast medium for gastrointestinal tract images by magnetic resonance imaging. Magnetic resonance imaging. 2006 Feb 1;24(2):195-200. DOI: 10.1016/j.mri.2005.10.026.

45. Cordova-Fraga T, Sosa M, Hernandez-Gonzalez MA, Reyes-Aguilera JA, Solorio S, Ramirez C, Bautista-Flores E, Reynaga G, Avila-Rodriguez M, De la Roca-Chiapas JM. Medlar (Achras sapota L.) as oral contrast agent for MRI

of the gastrointestinal tract. Applied Magnetic Resonance. 2012 Mar; 42:161-7. DOI: 10.1007/s00723-011-0267-8.

46. Shi H, Liu C, Ding HY, Li CW. Magnesium sulfate as an oral contrast medium in magnetic resonance imaging of the small intestine. European Journal of Radiology. 2012 Mar 1;81(3): e370-5. DOI: 10.1016/j.ejrad.2011.11.049
47. Elsayed NM, Alsalem SA, Almugbel SA, Alsuhaimi MM. Effectiveness of natural oral contrast agents in magnetic resonance imaging of the bowel. The Egyptian Journal of Radiology and Nuclear Medicine. 2015 Jun 1;46(2): 287-92. DOI: 10.1016/j.ejrnm.2015.03.007
48. Faletti R, Gatti M, Di Chio A, Fronda M, Anselmino M, Ferraris F, Gaita F, Fonio P. Concentrated pineapple juice for visualisation of the oesophagus during magnetic resonance angiography before atrial fibrillation radiofrequency catheter ablation. European Radiology Experimental. 2018 Dec;2(1):1-6. DOI: 10.1186/s41747-018-0067-0.
49. Hapsari SJ, Latifah R, Muhaimin M. The role of black tea and pineapple juice as negative oral contrasts on magnetic resonance cholangiopancreatography (MRCP) examination. Journal of Vocational Health Studies. 2019 Mar;2(3):121-6. DOI: 10.20473/jvhs.V2.I3.2019.121-126.
50. Isnoviasih ST, Anwar MC, Indrati R, Wibowo GM, Masrochah S. International Journal of Allied Medical Sciences and Clinical Research (IJAMSCR). 2019 Des;7(3): 784-788.
51. Mohabir S, Pitcher RD, Perumal R, Goodier M. The eficacy of pineapple juice as a negative oral contrast agent in magnetic resonance cholangiopancreatography. SA Journal of Radiology. 2020 Jan 1;24(1):1-6. DOI: 10.4102/sajr.v24i1.1875.

52. Pinho KE, Gewehr PM, Pinho AC, Gusso AM, Goedert CA. Image Evaluation in Magnetic Resonance Cholangiopancreatography. In BIOSIGNALS. 2020; 4: 98-105. DOI: 10.5220/0008987200980105.

53. Utami HS, Mulyantoro DK, Fatimah F. Jasmine tea as a negative oral contrast agent in magnetic resonance cholangiopancreatography (MRCP). InJournal of Physics: Conference Series 2021 Jul 1 (Vol. 1943, No. 1, p. 012039). IOP Publishing. DOI: 10.1088/1742-6596/1943/1/012039.

54. Vesna C, Bojana T, Bozidarka J. The efficacy of pineapple juice as a negative oral contrast agent in magnetic resonance cholangiopancreatography. Journal of Medical Imaging and Radiation Sciences. 2022 Dec 1;53(4): S63. DOI: 10.1016/j.jmir.2022.10.216.

55. Suner SS, Sahiner M, Umut E, Ayyala RS, Sahiner N. Physically Crosslinked Chondroitin Sulfate (CS)–Metal Ion (M: Fe (III), Gd (III), Zn (II), and Cu (II)) Particles for Versatile Applications and Their Biosafety. Pharmaceuticals. 2023 Mar 23;16(4):483. DOI: 10.3390/ph16040483.

56. Islam MK, Baek AR, Yang BW, Kim S, Hwang DW, Nam SW, Lee GH, Chang Y. Manganese (II) Complex of 1, 4, 7-Triazacyclononane-1, 4, 7-Triacetic Acid (NOTA) as a Hepatobiliary MRI Contrast Agent. Pharmaceuticals. 2023 Apr 17;16(4):602. DOI: 10.3390/ph16040602.

57. European Food Safety Authority. Scientific Committee on Food Scientific Panel on Dietetic Products, Nutrition and Allergies. Tolerable Upper Intake Levels for Vitamins and Minerals. 2006.

58. Gavrila DE. 7. MAGNETIC PROPERTIES OF MATERIALS; 2014 Jan 1.

59. Food Standards Agency. Safe upper levels for vitamins and minerals. Report of Expert Group on Vitamins and Minerals; 2003 May.

60. Bacchetta J, Edouard T, Laverny G, Bernardor J, Bertholet-Thomas A, Castanet M, Garnier C, Gennero I, Harambat J, Lapillonne A, Molin A.

Vitamin D and calcium intakes in general pediatric populations: A French expert consensus paper. Archives de Pédiatrie. 2022 May 1;29(4):312-25. DOI: 10.1016/j.arcped.2022.02.008.

61. World Health Organization. Vitamin and mineral requirements in human nutrition. World Health Organization; 2004.
62. Sarla GS. Calcium Supplementation: A Review of Oral Calcium Intake on Human Health. Open Acc J Oncol Med 3 (1)-2019. OAJOM. MS. ID.;151. DOI: 10.32474/OAJOM.2019.03.000151.
63. Hathcock JN. Vitamin and Mineral. Council for Responsible Nutrition; 2014.
64. Reid IR, Bristow SM, Bolland MJ. Calcium supplements: benefits and risks. Journal of internal medicine. 2015 Oct;278(4):354-68. DOI: 10.1111/joim.12394.
65. Olczak-Pruc M, Szarpak L, Navolokina A, Chmielewski J, Panasiuk L, Juárez-Vela R, Pruc M, Swieczkowski D, Majer R, Rafique Z, Peacock FW. The effect of zinc supplementation on the course of COVID-19–A systematic review and meta-analysis. Annals of Agricultural and Environmental Medicine. 2022 Dec 27;29(4):568-74. DOI: 10.26444/aaem/155846.
66. McMillen SA, Dean R, Dihardja E, Ji P, Lönnerdal B. Benefits and Risks of Early Life Iron Supplementation. Nutrients. 2022 Oct 19;14(20):4380. 0. DOI:10.3390/ nu14204380.
67. National Institutes of Health. Potassium Fact Sheet for Consumers. Office of Dietary Supplements;2019 Mar 5.
68. Dickinson HO, Nicolson D, Campbell F, Beyer FR, Mason J. Potassium supplementation for the management of primary hypertension in adults. Cochrane Database of Systematic Reviews. 2006(3). DOI: 10.1002/14651858.CD004641.pub2.

69. Vermeulen EA, Vervloet MG. Magnesium Administration in Chronic Kidney Disease. Nutrients. 2023 Jan 20;15(3):547. DOI: 10.3390/nu15030547

70. Haugen M, Lillegaard IT, Strand TA, Frøyland L, Holvik K, Løvik M, Tell GS, Iversen PO. Risk assessment of magnesium in food supplements. Opinion of the Panel on Nutrition, Dietetic Products, Novel Food and Allergy of the Norwegian Scientific Committee for Food Safety. VKM Report. 2016.

71. on Nutrition EP, Foods N, NDA FA, Turck D, Castenmiller J, de Henauw S, Hirsch-Ernst KI, Kearney J, Knutsen HK, Maciuk A, Mangelsdorf I. Dietary reference values for sodium. EFSA Journal. 2019 Sep;17(9). DOI: 10.2903/j.efsa.2019.5778.

72. Dietary Guidelines Advisory Committee. Dietary guidelines for Americans 2015-2020. Government Printing Office; 2015 Dec 31.

73. World Health Organization. Guideline: Sodium intake for adults and children. World Health Organization; 2012.

74. O'Donnell M, Mente A, Rangarajan S, McQueen MJ, Wang X, Liu L, Yan H, Lee SF, Mony P, Devanath A, Rosengren A. Urinary sodium and potassium excretion, mortality, and cardiovascular events. New England Journal of Medicine. 2014 Aug 14;371(7):612-23. DOI: 10.1056/NEJMoa1311889.

75. Gurol KC, Aschner M, Smith DR, Mukhopadhyay S. Role of excretion in manganese homeostasis and neurotoxicity: A historical perspective. American Journal of Physiology-Gastrointestinal and Liver Physiology. 2022 Jan 1;322(1): G79-92. DOI:10.1152/ajpgi.00299.2021.

76. National Institutes of Health. Manganese. Fact Sheet for Health Professionals; 2021.

77. Shrestha J. P-Value: A true test of significance in agricultural research; Oct 2019. DOI: 10.5281/zenodo.4030711.

78. Gupta SC, Gupta I. Business Statistics. Himalaya publishing house; 2008.

79. Weiers RM. Introduction to business statistics. Cengage Learning; 2010 Mar 17.
80. Taherdoost H. What is the best response scale for survey and questionnaire design; review of different lengths of rating scale/attitude scale/Likert scale. Hamed Taherdoost. 2019 Mar 29:1-0.
81. Schrum M, Ghuy M, Hedlund-Botti E, Natarajan M, Johnson M, Gombolay M. Concerning trends in likert scale usage in human-robot interaction: Towards improving best practices. ACM Transactions on Human-Robot Interaction. 2023 Apr 15;12(3):1-32. DOI: 10.1145/3572784
82. Kittel C. Introduction to solid state physics. John Wiley & sons, inc; 2005.
83. Martin, W. C., Musgrove, A., Kotochigova, S., & Sansonetti, J. E. (2011). Ground Levels and Ionization Energies for the Neutral Atoms (version 1.3). National Institute of Standards and Technology, Gaithersburg, MD.[Online] Available: http://physics. nist. gov/IonEnergy.
84. Heinrich FC, Schmidt V, Schramm M, Mertineit M. Magnetic and mineralogical properties of salt rocks from the Zechstein of the Northern German Basin. Geophysical Journal International. 2017 Mar;208(3):1811-31. DOI: 10.1093/gji/ggw488

الخلاصة

إنّ الصعوبة في تحديد الجهاز الهضمي من الأنسجة والأعضاء الطبيعية الداخلية حدّ من فائدة التصوير بالرنين المغناطيسي في تصوير منطقة البطن. وبغية تعزيز رؤية هذه الأعضاء والتي يتعذر الوصول إليها، فإن استخدام المواد الكيميائية كعوامل تباين ضرورية لأعضاء معينة، مثل الجهاز الهضمي (GI). وعادةً ما تكون عوامل التباين باهظة الثمن ولها آثار جانبية وغير متوفرة أحيانا في المستشفيات العراقية. فالغرض من هذه الدراسة هو إيجاد عوامل تباين فموية بديلة يمكن استخدامها في تصوير الجهاز الهضمي بالرنين المغناطيسي. ويجب أن تكون عوامل التباين هذه متوفرة، بدون تأثيرات ضارة أو قليلة الضرر، وغير مكلفة، وتعمل على تغيير في شدة إشارة الماء أثناء تصوير الجهاز الهضمي بالرنين المغناطيسي لتنتج تباينًا عاليًا وبأفضل جودة للصورة.

وتتلخص طريقة العمل في جمع المكملات المعدنية: مثل (الحديد والمغنيسيوم والبوتاسيوم والكالسيوم والزنك والصوديوم والمنغنيز) ثمَّ طحن وإذابة كل مكمل معدني (مقدار جرعة يومية) بكميات مختلفة من الماء المقطر (0.5 ،1، 1.5 ،2 كوب) للحصول على محاليل بتراكيز مختلفة (عينات). تمّ فحص العينات في التصوير بالرنين المغناطيسي باستخدام انابيب اختبار لتحديد العينة التي لديها أقل مستوى تركيز وأفضل جودة للصورة من ناحية الكمّية والنّوعية،

تشير نتائج الدراسة المختبرية إلى أن مكملات المغنيسيوم والبوتاسيوم والصوديوم ليس لها أي تأثير فعليٍّ على شدة إشارة الماء في صور T1-weightedوصور T2-weighted، في حين أن مكملات الكالسيوم عملت على زيادة شدة إشارة الماء في صور T2-weighted ، بينما تزيد مكملات المنغنيز والحديد من شدة إشارة الماء على T1-weightedمع تقليل شدة إشارة الماء على T2-weighted. بعد ذلك تم اختبار مكمل الكالسيوم والمنغنيز والحديد على المتطوعين.

خضع ثلاثون شخصًا أصحاء لفحص التصوير بالرنين المغناطيسي قبل وبعد الحصول على محلول المكمل معدني، حيث تم تقسيمهم إلى ثلاث مجموعات، في كل مجموعةٍ منها عشرة أشخاص، المجموعة الاولى تم إعطاؤهم مكملات الكالسيوم، والثانية مكملات المنغنيز، والثالثة مكملات الحديد، ويتم تقييم صور

الرنين المغناطيسي للمتطوعين كميًا عن طريق قياس شدة الإشارة ونسبة الإشارة إلى الضوضاء (SNR) ونسب الإشارة إلى الضوضاء النسبية (RSN) والتباين (C)، كما يتم تقييمها نوعيًا بواسطة أخصائي الأشعة.

من نتائج القياسات الكمية والتقييم النوعي لصور الرنين المغناطيسي، يمكن استنتاج أن مكملات الكالسيوم يمكن استخدامها كعامل تباين إيجابي في التصوير T2-weighted. بينما تعمل مكملات المنغنيز والحديد كأفضل عامل تباين إيجابي على الصورT1-weighted وعامل تباين سلبي في الصور T2-weighted.

جامعة كربلاء

كلية العلوم

قسم الفيزياء

تحديد عوامل التباين الفموية المؤثرة في تصوير الجهاز الهضمي بالرنين المغناطيسي

اطروحة مقدمة إلى مجلس كلية العلوم / جامعة كربلاء وهي جزء من متطلبات نيل درجة الدكتوراه في علوم الفيزياء

من قبل

زينب عبد الله منخي

بأشراف

أ. د. خالد ابراهيم رياح **أ. د. احمد محمود عبد اللطيف**

1445هـ 2023م